DECISION TREE-BASED MACHINE LEARNING TO OPTIMIZE THE LAMINATE STACKING OF COMPOSITE CYLINDERS FOR MAXIMUM BUCKLING LOAD AND MINIMUM IMPERFECTION SENSITIVITY

H.N.R. Wagner[a], H. Köke[b], S. Dähne[b], S. Niemann[b], C. Hühne[a,b] and R. Khakimova[c]

[a]*Technical University Braunschweig, Institute of Adaptronic and Functional Integration, Langer Kamp 6, 38106 Braunschweig, Germany*
ro.wagner@tu-braunschweig.de

[b]*German Aerospace Center (DLR), Institute for Composite Structures and Adaptive Systems, Lilienthalplatz 7, 38108 Braunschweig, Germany*
christian.huehne@dlr.de

[c] *Fraunhofer institute, Open Hybrid LabFactory e.V., Hermann-Münch-Straße 2, 38440 Wolfsburg, Germany*
Regina.Khakimova@iwu.fraunhofer.de

Keywords: Buckling, robust design, knockdown factor, imperfection sensitivity, composite shell, postbuckling, optimization, machine learning, decision tree

Abstract

Launch-vehicle primary structures like cylindrical shells are increasingly being built as monolithic composite and sandwich composite shells. These imperfection sensitive shells are subjected to axial compression due to the weight of the upper structural elements and tend to buckle under axial compression. In the case of composite shells the buckling load and imperfection sensitivity depend on the laminate stacking sequence.

Within this paper multi-objective optimizations for the laminate stacking sequence of composite cylinder under axial compression are performed. The optimization is based on different geometric imperfection types and a brute force approach for three different ply angles. Decision tree-based machine learning is applied to derive general design recommendations which lead to maximum buckling load and a minimum imperfection sensitivity.

The design recommendation are based on the relative membrane, bending, in-plane shear and twisting stiffnesses. Several optimal laminate stacking sequences are generated and compared with similar laminate configurations from literature. The results show that the design recommendations of this article lead to high-performance cylinders which outperform comparable composite shells considerably. The results of this article may be the basis for future lightweight design of sandwich and monolithic composite cylinders of modern launch-vehicle primary structures.

Abbreviations and glossary

Exp.	Experiment
F	Axial Load
GNA	Geometrically nonlinear analysis
KDF	Knockdown factor
L	Cylinder length
MGI	Measured geometric imperfections
N	Buckling load in general
R	Radius of cylindrical shells
SBPA	Single boundary perturbation approach
SPCA	Single perturbation cutout approach
SPDA	Single perturbation displacement approach
SPLA	Single perturbation load approach
t	Wall thickness of cylindrical shells
t_{ply}	Ply thickness
u	Axial shortening
α	Ply angle
β	Ply angle
γ	Ply angle
ρ	knockdown factor

1 Introduction

Thin-walled shell structures, like cylinder are important structural elements for launch-vehicle systems. These shells are subjected to axial compression due to weight of the upper structural elements and propulsive loads during launch. Within this article, the maximum load carrying capability of thin-walled cylindrical shells under axial compression is defined as the buckling load.

Launch-vehicle primary structures are increasingly being built from fiber-reinforced composite materials [1]. These materials can have special advantages when compared to metals like high specific strength and stiffness as well as good environmental and fatigue resistance [2], [3].

Besides monolithic composite shell structures, sandwich composite structures which consist of a lightweight core and high strength and stiffness facesheets are also used as launch-vehicle primary structures [4].

A large number of composite cylinders were tested in order to understand buckling of composite shells under axial compression. The buckling results are shown in Fig. 1 by means of a knockdown factor (which is herein defined as a ratio of the experimental determined buckling load to the theoretical perfect buckling load) versus the radius-to-thickness ratio (R/t – shell slenderness or thinness). The experimental data collection in Fig. 1 (left) shows that there is a significant deviation between the buckling theory and the corresponding experimental results.

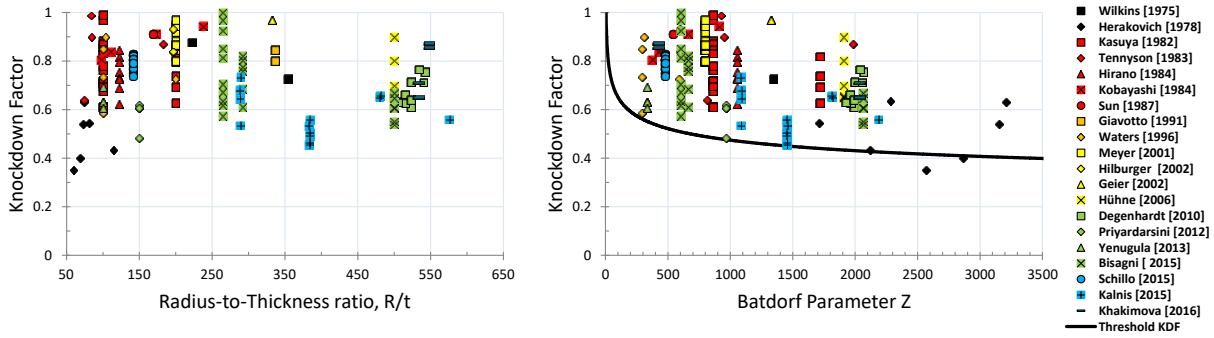

Fig. 1: Distribution of the experimental data of axial compressed cylindrical composite shells for different R/t ratios (left) and different Batdorf Parameter Z with Threshold design curve (right)

A main cause for the large discrepancy between buckling theory and experiment are geometric imperfections. Koiter [5] showed that geometric imperfections can reduce the buckling load of thin-walled shells significantly. Geometric imperfections are defined as shape deviations from the ideal structure. Depending on the shape and amplitude of the geometric imperfections; a single dimple appears within the shell during loading. This single dimple initiates the buckling process and occurs in thin-walled shells like cylinders [6], [7], cones [8] and spheres [9], [10]. A significant number of researchers investigated the influence of different geometric imperfections [11], like axisymmetric imperfection [12] and real measured imperfection [13], on the buckling load.

However, the buckling load of thin-walled shells is not only reduced by traditional geometric imperfections. But also by non-traditional imperfections like loading imperfections [14], [15] or delamination imperfections as recently shown by Wang et al. [16]. Loading imperfections are defined as the deviation from the perfect homogenous load introduction of a shell. There are several known different loading imperfections like local concentrated loading imperfections [17], [18] and uniform bending of the shell edge [19]. The buckling load reduces significantly if

loading imperfections occur which was shown in [20]. Therefore they have to be considered in the design process as well.
New design criteria for full-scale [21], [22] and sub-scale stiffened metal [23], [24] and sandwich composite shells [4], [25], [26] are currently being developed by NASA in the Shell Buckling Knockdown Factor Project (SBKF, references [27] and [28]). A detailed summary regarding the SBKF project is given in [29] and [30].
A similar project started 2012 in Europe, the DESICOS project [31] (new robust **DES**ign guideline for **I**mperfection sensitive **CO**mposite launcher **S**tructures) to develop and validate new deterministic [32], probabilistic [33] as well as experimental [34], [35] design approaches for composite shells [36], [37], [38], [39]. A comprehensive overview regarding this project is for example given in [2].
Recently, comprehensive imperfection sensitivity studies for cylindrical [25] and conical [40], [41] sandwich composite shells were published which indicate that the current NASA recommendations for composite shells may be very conservative for modern launch-vehicle structures. Consequently, it was suggested to investigate the buckling response of composite sandwich shells through buckling tests and analytical predictions. In order to perform less expensive and at the same time representative buckling tests for composite sandwich shells a new scaling methodology was proposed by Balbin et al. [42].
An alternative to buckling tests and analytical predictions are lower-bound methods like the single boundary perturbation approach (SBPA) [43], [8] or the worst multiple perturbation load approach (WMPLA) [44], [45]. The SBPA is a numerical design approach which is realized using finite element simulations [46], [47]. The advantage of this methodology is that no information regarding imperfections measurements are required [48]. This method can also be used to study the imperfection sensitivity of composite shells which was shown extensively in [49]. Studies in [50] show that the SBPA delivers robust (conservative with respect to experimental results) lower-bounds for composite shells which lead to a new design load bound for thin-walled composite cylinders which is given by equation (1):

$$\rho_{TH} = \Omega_{\mathrm{TH}} \cdot (R/t)^{-\eta_{TH}} \tag{1}$$

$$\Omega_{\mathrm{TH}} \approx -0.0196 \cdot \left(\frac{\mathrm{L}}{\mathrm{R}}\right)^2 - 0.0635 \cdot \left(\frac{\mathrm{L}}{\mathrm{R}}\right) + 1.3212\,, \quad 1 \leq L/R \leq 3 \tag{2}$$

$$\eta_{\mathrm{TH}} \approx -0.013 \cdot \left(\frac{\mathrm{L}}{\mathrm{R}}\right)^2 + 0.061 \cdot \left(\frac{\mathrm{L}}{\mathrm{R}}\right) + 0.08\,, \quad 1 \leq L/R \leq 3$$

Evkin [51] proposed to express equation (1) by using the Batdorf parameter Z, see equation (3-4). A comparison with experimental results in Fig. 1 (right) shows that the modified lower-bound by Evkin delivers conservative lower-bound estimates for Z ~ 300-2500.

$$\rho_{TH} = 1.23 \cdot (Z)^{-0.138}, \quad 50 \leq Z \leq 7000 \tag{3}$$

$$\mathrm{Z} = \frac{\mathrm{L}^2 \cdot \sqrt{(1-v^2)}}{R \cdot t} \tag{4}$$

In the case of composite shells, the buckling load [52], [53] as well as the imperfection sensitivity [54] also depend on the laminate stacking sequence. Those results were validated within the BRITE-EURAM-project "Design and Validation of Imperfection-Tolerant Laminated Shells" (DEVILS) [55], [56].
First studies which optimized the ply-layup of axially loaded composite cylinders for maximum buckling load were published by Khot [57], Tennyson and Hansen [58] as well as Hirano [59]. Studies by Onoda [60] have shown that there are many optimal laminate configurations, both symmetric and asymmetric. The optimization of the maximum buckling load for a composite cylinder is a formidable task due to the presence of many local maxima which was highlighted by Nshanian and Pappas [61]. The maximum buckling load for a composite cylinder may be

based on quasi-isotropic laminate stacking which was shown by Todoroki [62]. Most optimization studies didn't consider the influence of imperfections on the buckling load. However, studies by Hühne [63] and Elishakoff [64] have shown that the optimization for maximum buckling load and minimum imperfection sensitivity may lead to more reliable composite shell configurations than optimization for only the maximum buckling load.
The purpose of this article is to derive general design recommendation for the laminate stacking sequence of high-performance (high buckling load and low imperfection sensitivity) composite cylinder under axial compression.
In the second section of this article, the numerical model is presented and different imperfection measures are introduced. In the subsequent third section, the influence of different imperfection measures on the buckling load of composite cylinders is investigated. Based on the results of section 3 an imperfection measure is chosen to optimize a realistic laminate stacking with three different ply angles for maximum buckling load and minimum imperfection sensitivity in section 4. Furthermore, a machine learning algorithm is used to evaluate the multi-objective optimization results of section 4 and to derive general design recommendations for composite cylinders under axial compression. In section 5, the design recommendation are applied to derive laminate configurations for monolithic composite cylinders with five different ply angles. The corresponding shells are analyzed and compared with optimized shells from literature.

2 Geometric imperfection and lower-bound analysis of axially loaded cylinders

In this section the numerical model is presented and different imperfection measures are introduced and described in detail.

2.1 Numerical model

In this section, the numerical model for the optimization is presented and described. The investigated shells have a radius R = 250 mm, a free length L = 500 mm, a wall thickness t = 0.5 mm and a ply thickness of t_{ply} = 0.125 mm. The material parameters for the composite shells are given in Table 1. The composite shells are modeled by using linear shell elements (S4R in ABAQUS [65]) and the finite element length was defined as 5.6 mm according to $0.5\sqrt{Rt}$ [66].

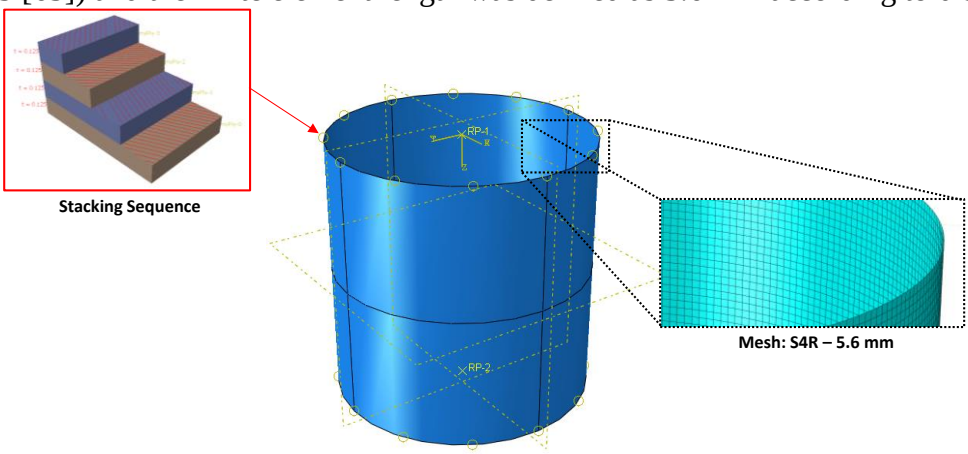

Fig. 2: Numerical model of the cylinder

The mechanical boundary conditions on both cylinder edges are defined as clamped by using rigid-body interactions which are coupled with a reference point. The displacement in axial the direction is free at the top cylinder edge for load application. Geometrically nonlinear analyses (GNA) are performed in ABAQUS [65] in order to determine the buckling load.

Table 1: Material properties of the investigated cylindrical shells after [52]

Material parameter	Dimension
elasticity modulus E_{11} - [MPa]	125774
elasticity modulus E_{22} - [MPa]	10030
Poisson's ratio ν_{12} - [-]	0.271
shear modulus G_{12} - [MPa]	5555

2.2 Geometric imperfection and lower-bound methods

The buckling load of the perfect (without imperfections) and of the imperfect cylindrical shell depends on the laminate stacking sequence which was shown by Geier [56] and Hirano [59]. Studies by Hühne [15], Kriegesman [67] and Friedrich [68] indicate that the laminate stacking sequence of a composite shell which results in the maximum perfect buckling load is different to the laminate stacking sequence which results in the maximum imperfect buckling load. In order to verify the results of the before mentioned authors two different composite cylinders are now presented and analyzed.

The shells were defined according to optimization studies by Zimmerman [52] and built, studied as well as tested by Hühne [63]. The first shell is denominated as Z07 and has the laminate stacking sequence [24,-24, 41,-41] which results in the maximum perfect buckling load for a [α,−α, β,−β] laminate, see Fig. 3 (left). The second shell is denominated as Z09 and has the reversed stacking sequence of Z07 [41,-41, 24,-24] which leads to a very low imperfection sensitivity but also a low buckling load, as shown in Fig. 3 (right).

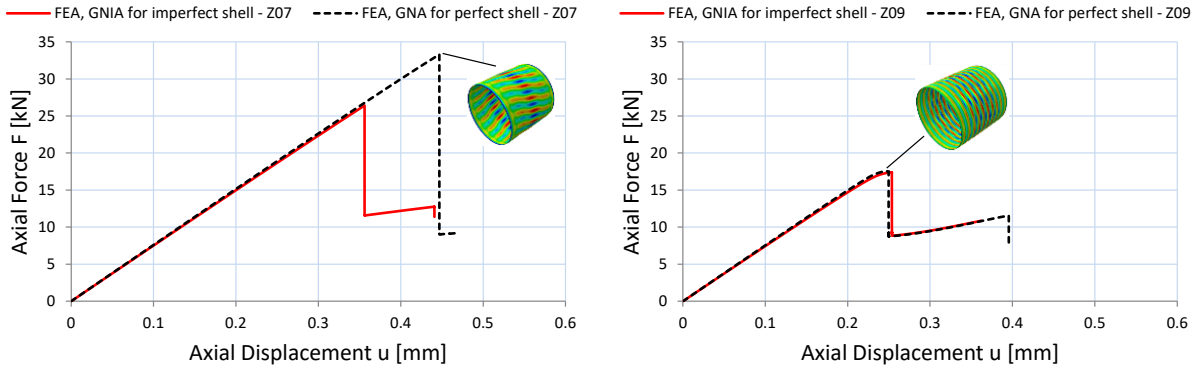

Fig. 3: Load displacement curves for the shells Z07 and Z09 according to a GNA and GNIA (with measured geometric imperfections)

In order to study the imperfection sensitivity of both shells, different methods are presented and applied in the following. The shell surface of the test specimens Z07 and Z09 were measured with the optical measurement system ARAMIS and the resulting point cloud was converted to a finite element mesh with the software VISTIM [63]. This imperfection type is commonly defined as measured geometric imperfection (MGI) and allows to analyze the influence of manufacturing specific and realistic geometric imperfections on the buckling load.
The MGI of Z07 and Z09 are shown in Fig. 4 and lead to a 23 % reduction of the buckling load in the case of Z07 and a 1 % reduction for the buckling load of Z09 as shown in Fig. 3.

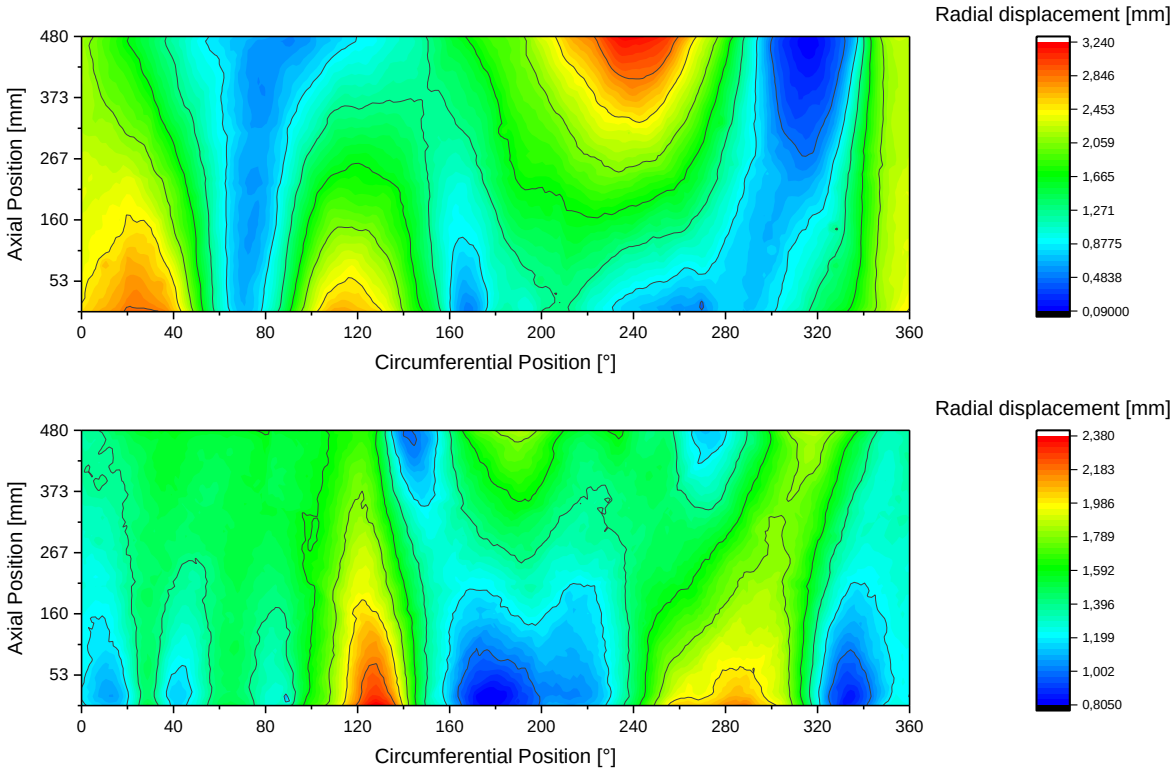

Fig. 4: Measured midsurface radial deviations from a best-fit cylinder for the shell Z07 (top) and Z09 (bottom)

The application of MGI is most of the time not suitable because it requires already built structures which have to be measured. Also, real shell structures may be burdened by multiple different imperfection types like inhomogeneous loading around the circumference, cutouts or wall thickness deviations and delamination.

Therefore the application of only MGI may result in non-conservative design load estimations. In order to be independent from imperfection measurements and cover the influence of multiple or large amplitude imperfections, different lower-bound methods have been developed as shown in Fig. 5.

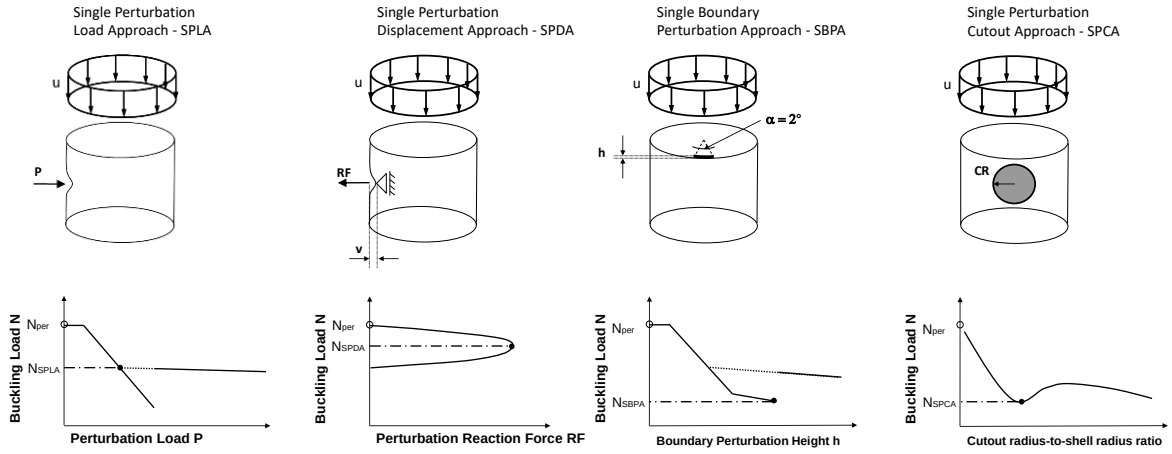

Fig. 5: Perturbation concepts for the design of cylinders under axial compression: SPLA, SPDA, SBPA and SPCA (from left to right)

Lower-bound methods should deliver a theoretical plateau for the buckling load which is equal or less to every buckling load caused by multiple or large-amplitude imperfections. One of the first realistic lower-bound methods was proposed by Hühne et al. [14], the single-perturbation

load approach (SPLA) causes a dimple imperfection in a cylinder by means of a lateral perturbation load Fig. 5 (left). The amplitude of the dimple imperfection is increased by increasing the magnitude of the lateral perturbation load P.
The buckling load decreases as the perturbation load is increased until a specific plateau for the buckling load can be determined. The plateau is due to the membrane stress redistribution in the cylinder. Large-amplitude dimple imperfections lead to snap-through buckling which leads to local buckling of the cylinder surface and reduces the membrane stresses above and below the snap-through to approximately zero, therefore a further increase of the perturbation load doesn't lead to a further reduction of the buckling load.
The design load of the SPLA is defined according to Fig. 5 (left) as the first buckling load in the plateau range, the corresponding KDFs for the shells Z07 and Z09 are given in Table 2 and shown in Fig. 6 (right). The SPLA leads to a 40 % reduction of the buckling load of Z07 and a 10 % reduction for Z09.

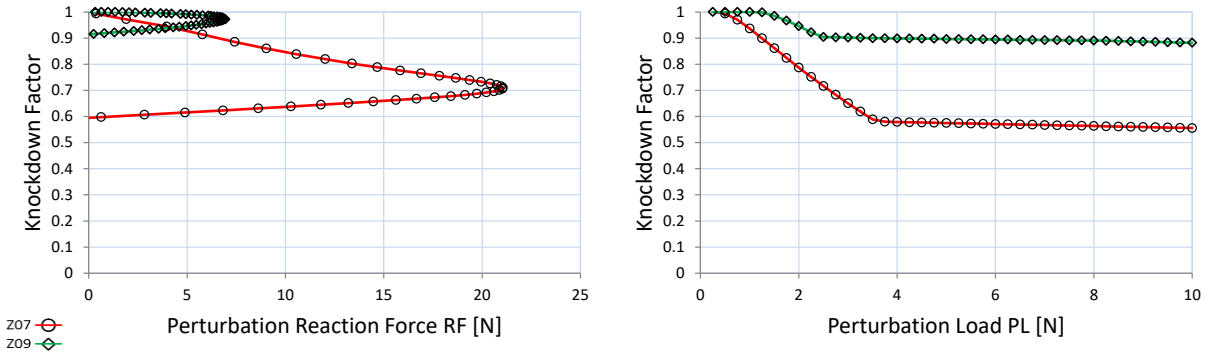

Fig. 6: Buckling load vs. perturbation reaction force according to the SPDA (left) buckling load vs. perturbation load according to the SPLA (right)

Modern manufacturing techniques for aerospace applications deliver high quality shells nowadays which don't have large-amplitude imperfections and result in a significantly lower buckling load reduction as shown in studies by NASA [21] and the Dalian University of Technology [69], [70].
High quality shells may not suffer from snap-through buckling and a method which allows the quantification of the pre-snap-through imperfection sensitivity was developed by Wagner et al. [20]. The single-perturbation displacement approach (SDPA) [50] relies on displacement controlled indentations to approximate the limit load for snap-through buckling as shown in Fig. 5 (middle left). The buckling load reduction according to the SPDA is 29 % for Z07 and 3 % for Z09.
Deviations from the perfect homogenous loading of the shell may also lead to snap-through buckling although the shell geometry has a high manufacturing quality. A method which allows the quantification of snap-through buckling due to localized loading imperfections was developed by Wagner et al. in [49]. The single boundary perturbation approach (SBPA) [46] causes a dimple imperfection near the loading edge by means of a localized uneven shell edge as shown in Fig. 5 (middle right). For large-amplitude dimple imperfections, the snap-through induced local buckling event may cause early global collapse of the shell which was validated in [46] and shown with nonlinear dynamic simulations in [71]. Therefore, the minimum local buckling load is defined as design load within the framework of the SBPA. The buckling load reduction according to the SBPA is 56 % for Z07 and 24 % for Z09 as shown in Fig. 7 (left).
Another, lower-bound method is based on cutouts. First studies which show that cutouts lead to a lower-bound for the buckling load were summarized Starnes [72] and the application of cutouts as an equivalent geometric imperfection was proposed by Wagner et al. [48].

Cutouts lead to a similar structural behavior as the local snap-through, the membrane stresses above and below the cutout are approximately zero (if the cutout is large enough) and the local buckling load approaches a plateau although the radius of the cutout increases as shown in Fig. 5 (right). The minimum local buckling load of the SPCA lead to similar KDFs for the buckling load as the SBPA as shown in Fig. 7. The buckling load reduction according to the SPCA is about 57 % for Z07 and 23 % for Z09.

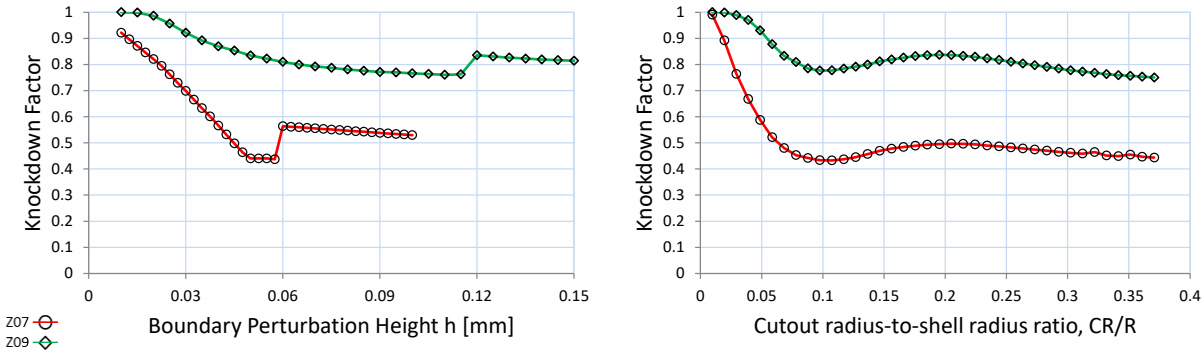

Fig. 7: Buckling load vs. edge perturbation according to the SBPA (left) buckling load vs. cutout to shell radius ratio according to the SPLA (right)

Yet another measure for the imperfection sensitivity is the post-buckling load of the perfect shell. Studies in [73] show that the post-buckling load gives good approximations for early shell buckling experiments and may be considered as the absolute worst case buckling scenario. Both shells have the same post-buckling load of about 9 kN but different KDFs as shown in Table 2 and Fig. 3. In every case the shell Z07 has a lower KDF for the buckling load compared to the shell Z09. However, the imperfect buckling load of Z07 is still higher. The test buckling load of Z07 was about 25 % higher compared to the test buckling load of Z09.

Table 2: Comparison of buckling loads and KDFs for the composite cylinder Z07 and Z09

Shell	**Z07**	**Z09**
Buckling Load [kN]		
GNA	33.29	17.52
Knockdown factors (KDF)		
MGI	0.793	0.992
SPDA	0.710	0.971
SPLA	0.597	0.904
SBPA	0.436	0.762
Cutout	0.432	0.777
Post	0.275	0.505
Experiment	0.648	0.896

3 Influence of the laminate stacking on the buckling load of composite cylinders

The purpose of this section is to identify an imperfection measure which is suitable for the optimization of a realistic laminate stacking sequence of composite cylinders under axial compression for maximum buckling load and minimum imperfection sensitivity.
For this purpose, the laminate stacking sequence $[\pm\alpha, \pm\beta]$ is analyzed; similar to studies in [15]. The ply angles α and β are varied in 5°-steps from 0°-90°, which results in 361 different shell configurations. In a first step the influence of the laminate stacking on the buckling load without imperfections is studied (perfect shell). In the second section, composite cylinders with optimized laminate stacking sequence for maximum buckling load from literature are presented and analyzed. In the third section, different lower-bound and geometric imperfection methods are used to study the influence of the laminate stacking on the imperfect buckling of axially loaded composite cylinder. The last section ends with a summary of the main results.

3.1 Perfect shell analysis

In this section the influence of the laminate stacking on the buckling load of the perfect shell (without imperfections) is studied and important laminate stiffness parameter are introduced. The buckling load N_{GNA} of a shell without imperfections obtained by a geometrically nonlinear analysis (GNA) is shown in Fig. 8 (left) and the corresponding axial displacement u_{GNA} is shown in Fig. 8 (right) for composite cylindrical shells with different laminate stacking sequences $[\pm\alpha, \pm\beta]$.

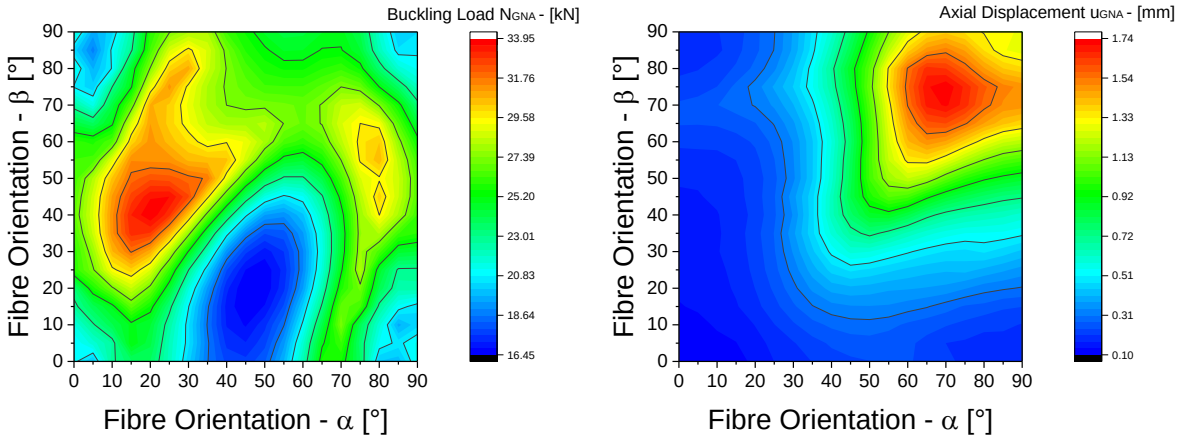

Fig. 8: Buckling load N_{GNA} (left) and axial displacement u_{GNA} (right) of the perfect shell structure for different laminate stacking sequences

The relative membrane and bending stiffnesses affect the buckling response and the imperfection sensitivity of a cylindrical shell; therefore several nondimensional parameters are used in order to assess the shell design. The first parameters are the axial-to-circumferential membrane and bending stiffness ratios, A_{11}/A_{22} and D_{11}/D_{22}, which are used as a measure of layup tailoring. These parameter ratios will be greater than unity for axially stiff cylinders, less than unity for circumferentially stiff cylinders; and will be unity for (quasi)isotropic cylindrical shells. Both stiffness ratios are equal for the [±α, ±β] layup shells as shown in Fig. 9.

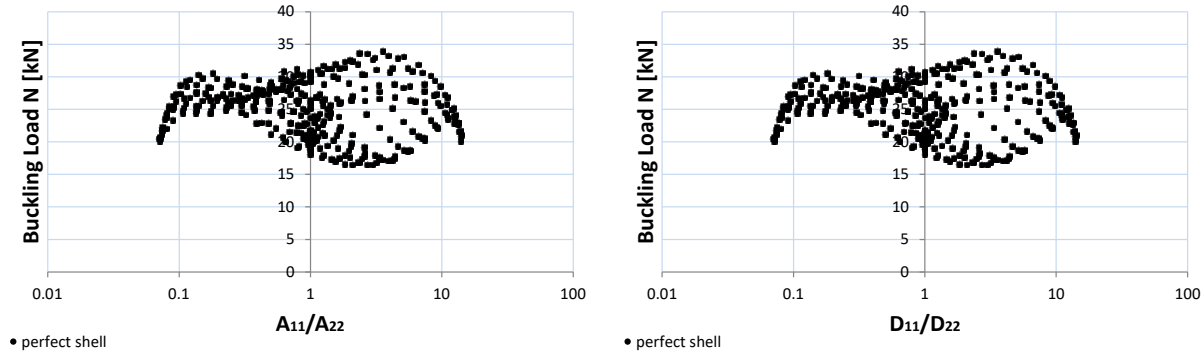

Fig. 9: Buckling load vs. axial-to-circumferential membrane stiffness ratio (A_{11}/A_{22}) – left – and bending stiffness ratio (D_{11}/D_{22}) – right – for the $[\pm\alpha, \pm\beta]$ shells

Axially stiff composite shells (A_{11}/A_{22} >1) with a high perfect buckling load can be identified at $[\pm 20, \pm 45]$. The reversed stacking sequence of the axially-stiff composite shells $[\pm 45, \pm 20]$ results in low perfect buckling loads. Circumferentially stiff composite shells (A_{11}/A_{22} <1) with a high perfect buckling load can be identified at $[\pm 75, \pm 45]$.

These results correspond with a finding made by Geier [56] who stated that the presence and the position of [+45,-45] plies strongly influences the buckling load. External placed plies [+45,-45] result in a high perfect buckling load and internal placed [+45,-45] plies lead to low perfect buckling loads.

The in-plane shear and twisting stiffnesses, A_{66} and D_{66} and can vary greatly for laminated composite shells and are represented by means of the nondimensional stiffness parameters given by equation:

$$\underline{A}_{66} = \frac{A_{66} \cdot A_{66}}{A_{11} \cdot A_{22}}$$

$$\underline{D}_{66} = \frac{D_{66} \cdot D_{66}}{D_{11} \cdot D_{22}} \tag{5}$$

For this case both stiffness ratios are also equal for the [±α, ±β] layup shells, see Fig. 10.

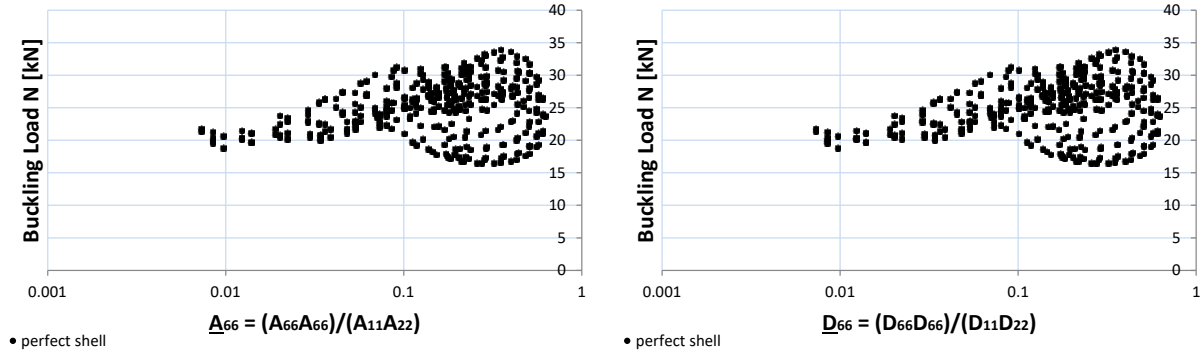

Fig. 10: Buckling load vs. in-plane shear stiffness to axial and circumferential membrane stiffness – left – and in-plane twisting stiffness to axial and circumferential bending stiffness – right – for the $[\pm\alpha, \pm\beta]$ shells

These parameters will be approximately 0.12 for isotropic materials with Poisson's ratio ν = 0.3 and for sandwich shells with quasi-isotropic facesheets. Sandwich shells with cross-ply facesheets have values less than 0.12.

3.2 Maximum buckling load composite cylinders

In this section different optimized laminate stacking sequences for maximum buckling load of composite cylinders under axial compression are compared and discussed. Hühne [15] applied the SPLA to determine the maximum imperfect buckling load of cylindrical composite shells which resulted in $[\pm 25,90,90]$, see Table 3. The second composite shell in this section was designed by Zimmerman [52], who assumed that the maximum buckling load of the perfect shell $[\pm 24, \pm 41]$ also leads to the maximum buckling load of the imperfect shell, see Table 3. Friedrich [68] determined the maximum imperfect buckling load by using an axisymmetric imperfection that results in the laminate stacking sequence $[\pm 34, \pm 49]$. The forth shell was designed by Kriegesmann [67] by using probabilistic methods with measured geometric imperfections and loading imperfections (rotation of the upper loading plane) and has the laminate stacking sequence $[\pm 78.75, \pm 67.5]$.

Table 3: Laminate stacking sequence for the composite shells and corresponding buckling load of perfect shell

Shell	ply-layup	Method / Imperfection model	A_{11}/A_{22}	$\underline{A}_{66}$	N_{GNA} [kN]
Hühne [15]	$[\pm 25, \pm 90]$	geometric dimple imperfection (SPLA)	0.70	0.05	26.04
Zimmerman [52]	$[\pm 24, \pm 41]$	max. perfect shell	3.01	0.41	32.73
Friedrich [68]	$[\pm 34, \pm 49]$	rotational symmetric geometric imperfections	1.38	0.50	31.46
Kriegesmann [67]	$[\pm 78.75, \pm 67.5]$	measured geometric imperfections and bending	0.10	0.17	28.43

The load-displacement curves of all presented shells are shown in Fig. 11 and the buckling loads according to a GNA (perfect shell) are given in Table 3.

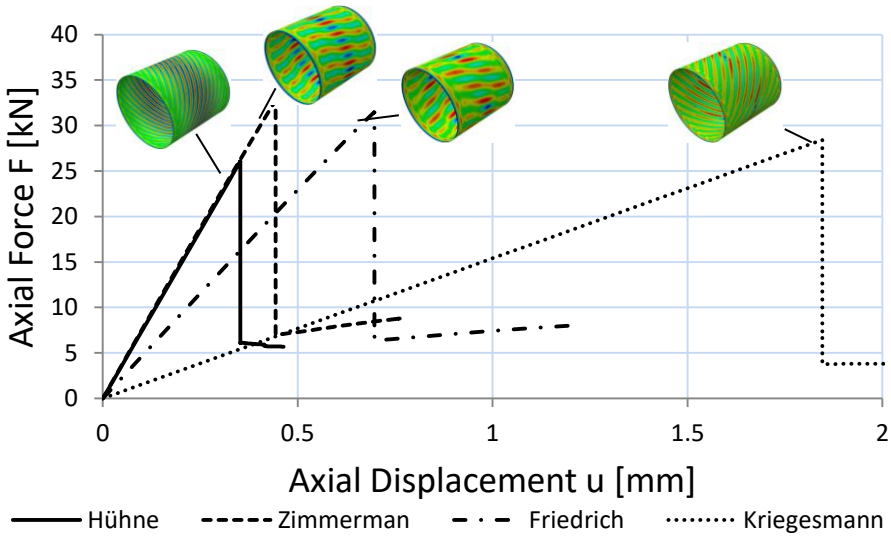

Fig. 11: Load-displacement curve of different composite shells

The results show that the shell $[\pm 25, \pm 90]$ has a similar axial stiffness as the shell which was designed by Zimmermann $[\pm 24, \pm 41]$ although both designs have significantly different A_{11}/A_{22} ratios. The shell design by Friedrich $[\pm 34, \pm 49]$ has a lower axial stiffness and nearly the same perfect buckling load as the shell by Zimmermann. The shell by Kriegesmann has the lowest axial stiffness and also the lowest A_{11}/A_{22} ratio of all four shells.

3.3 Imperfect shell analysis

In this section different design and lower-bound methods (from section 2) are applied in order to study the influence of the laminate stacking sequence on buckling load of an axially loaded composite cylinder with imperfections.
The imperfect buckling loads for different laminate stacking sequences according to the SBPA and the corresponding knockdown factor is shown in Fig. 12. There is one distinct maximum and one distinct minimum for the lower-bound buckling load (see Fig. 12 - left). Circumferentially-stiff shells have a significantly lower minimum buckling load as axially stiff composite shells.

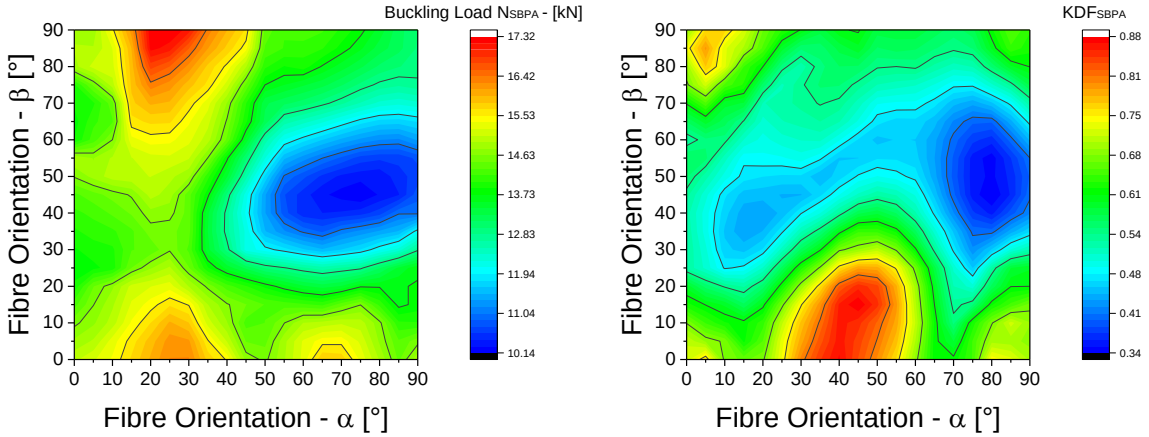

Fig. 12: Lower-bound buckling load (right) and knockdown factor (left) for different laminate stacking sequences: SBPA

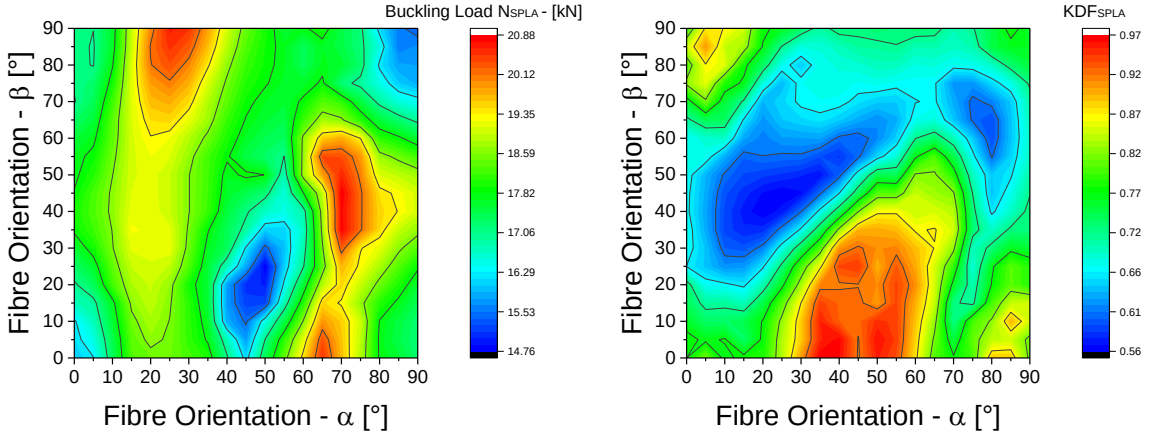

Fig. 13: Lower-bound buckling load (right) and knockdown factor (left) for different laminate stacking sequences: SPLA

The composite shell with $[\pm 25, \pm 90]$ has the highest imperfect buckling load and the lowest imperfection sensitivity of all shells. This laminate stacking sequence was also identified with the single perturbation load approach (SPLA) by Hühne [15]. The results of the SPLA are shown in Fig. 13 for the purpose of comparison. The design load of the SPLA is the first global buckling load which overestimates the lower-bound buckling load of the SBPA (minimum local buckling load) for circumferentially-stiff shell significantly.
Similar contour plots for different buckling loads like the design loads according to the single perturbation displacement approach (SPDA) and simulations with measured geometric imperfection (MGI) are shown in Fig. 14 - Fig. 15. The results show that the maximum imperfect buckling load N_{SPDA} has a laminate stacking sequence of $[\pm 20, \pm 30]$.

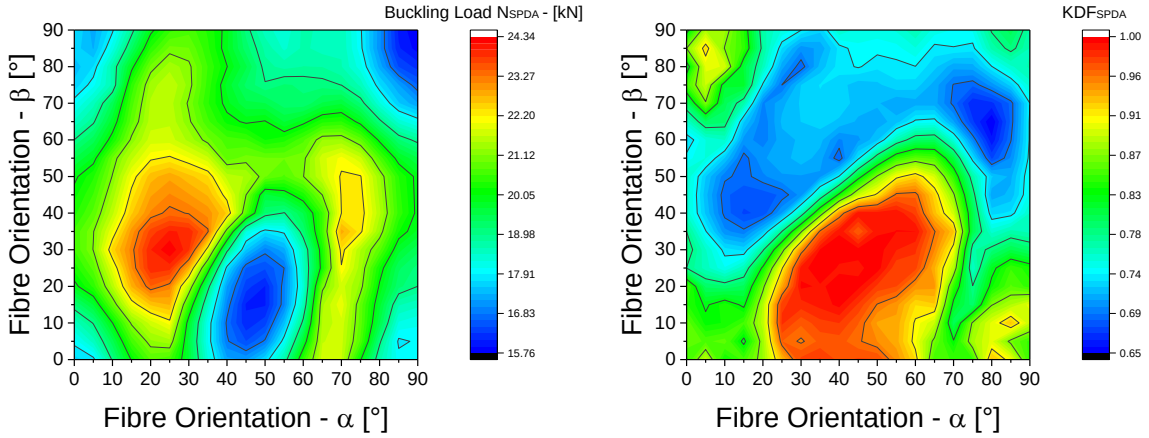

Fig. 14: Lower-bound buckling load (right) and knockdown factor (left) for different laminate stacking sequences: SPDA

Next, the influence of real measured imperfection on the buckling load is studied. The real measured imperfections were defined by a double Fourier series [74], [75] and are based on measurements from [33] (mean of ten different geometric imperfection patterns from ten nominal identical cylinders with $[\pm 24, \pm 41]$). The maximum imperfect buckling load N_{MGI} corresponds to a stacking sequence of $[\pm 30, \pm 50]$ and the lowest imperfect buckling loads correspond $[\pm 45, \pm 20]$ (similar to the SPDA).

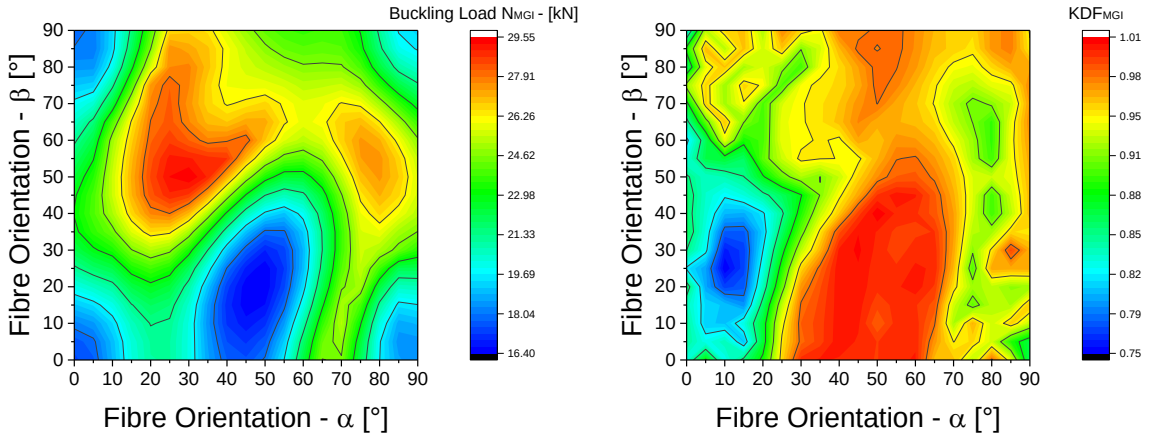

Fig. 15: Imperfect buckling load (right) and knockdown factor (left) for different laminate stacking sequences: MGI

Cutouts in a cylinder (positioned right in the middle between the cylinder boundaries) can also be used to determine a reasonable lower-bound buckling load and the corresponding results are shown in Fig. 16. The highest imperfect buckling loads can be determined at $[\pm 10, \pm 20]$ and the lowest imperfect buckling loads corresponds to shells with $[\pm 80, \pm 90]$.

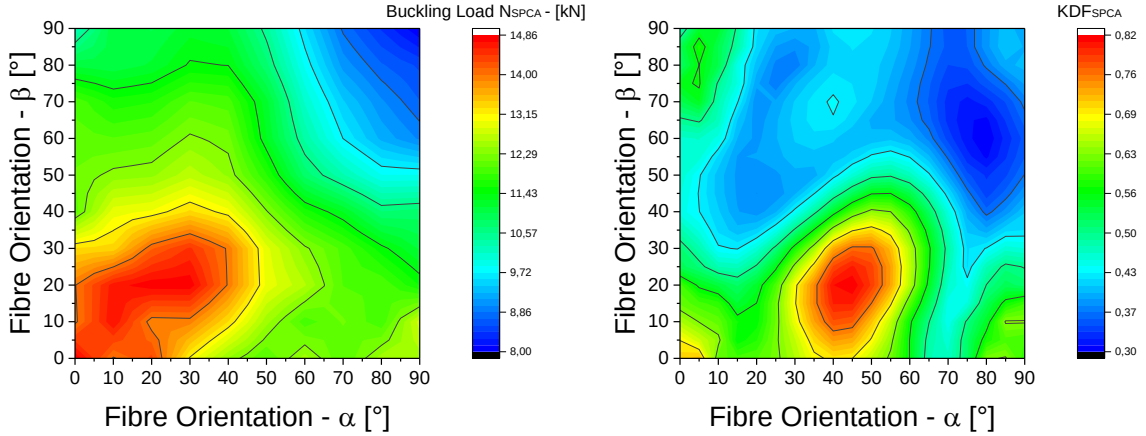

Fig. 16: Lower-bound buckling load (right) and knockdown factor (left) for different laminate stacking sequences: SPCA

According to Esslinger [76], the post-buckling load can also be considered as a measure for the imperfection sensitivity of a cylinder, see Fig. 17. The highest post-buckling load corresponds to the ply layup $[\pm 30, \pm 30]$ and circumferential-stiff (A_{11}/A_{22} <1) shells have the lowest post-buckling loads.

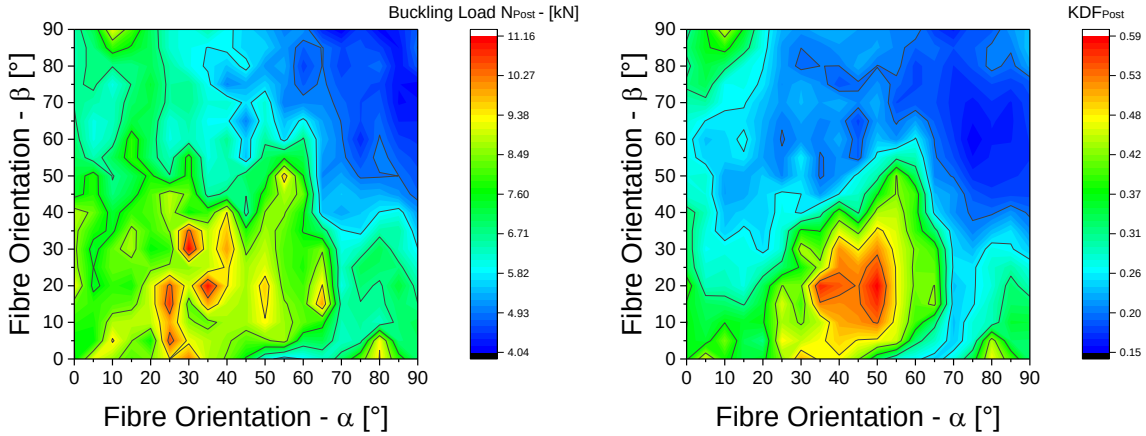

Fig. 17: Post-buckling load (right) and knockdown factor (left) for different laminate stacking sequences

3.4 Conclusion

In this final section, the four optimized shells from section 3.2 are compared in order to assess their imperfection sensitivity, see Fig. 18 and Table 4.
The shell design by Zimmerman has four times the highest buckling load (perfect shell, MGI, post-buckling and cutout) and the shell design by Hühne has two times the highest buckling load (SBPA and SPLA). The shell design by Friedrich has the third best overall imperfection sensitivity. The circumferential-stiff (A_{11}/A_{22} <1) shell by Kriegesmann has the worst overall imperfection sensitivity.
The results of this section indicate that it may not be necessary to optimize the imperfect buckling load but it is sufficient to optimize the perfect buckling load. The laminate stacking sequence for the maximum perfect buckling load $[\pm 24, \pm 41]$ has overall the best performance. The corresponding imperfect buckling load is even in the case of dimple imperfections (SBPA, SPLA) not much lower than the imperfect buckling load corresponding to the stacking sequence $[\pm 25, \pm 90]$. Based on these results the perfect buckling load according to a GNA and

the imperfect buckling load according to the SBPA are chosen for the optimization studies of section 4.

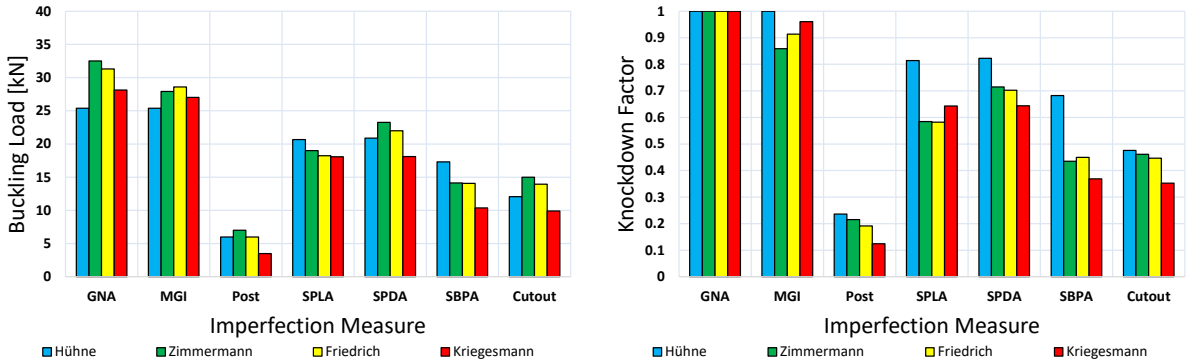

Fig. 18: Comparison of the buckling load and KDF for composite cylinders under axial compression with optimized stacking sequences from literature

Table 4: Comparison of optimized stacking sequences burdened by different imperfections with corresponding buckling loads in [kN]

Shell	Hühne [15]	Zimmerman [52]	Friedrich [68]	Kriegesmann [67]
Perfect shell (GNA)	26.04	**32.73**	31.46	28.43
MGI	25.61	27.91	**28.59**	27.02
Postbuckling	6.04	**7.09**	6.03	3.51
SPLA	**20.66**	18.99	18.22	18.09
SPDA	20.88	**23.24**	21.98	18.1
SBPA	**17.32**	14.14	14.07	10.38
Cutout	12.07	**14.99**	13.96	9.91
Best	2 times	4 times	1 time	0 times

4 Machine learning to optimize the laminate stacking for maximum buckling load

In this section the chosen imperfections measures from section 3 (perfect shell and SBPA) are applied to generate input data for the machine learning algorithm. Subsequently, decision tree-based machine learning is applied to derive general design recommendation for composite cylinder under axial compression.

4.1 Buckling Loads for composite cylinders with [α,–α,β,γ,γ,β,–α,α] laminate

In this section the maximum perfect and maximum imperfect buckling load of a symmetric ply layup $[\pm\alpha,\beta,\gamma]s$ is determined in order to define the input parameter for the machine learning algorithm using the scikit-learn decision tree classifier.
The ply angles α, β and γ are varied in 5°-steps from 0°-90°. The investigated shells have a radius R = 250 mm, a free length L = 500 mm, a wall thickness t = 1 mm and a ply thickness of t_{ply} = 0.125 mm.

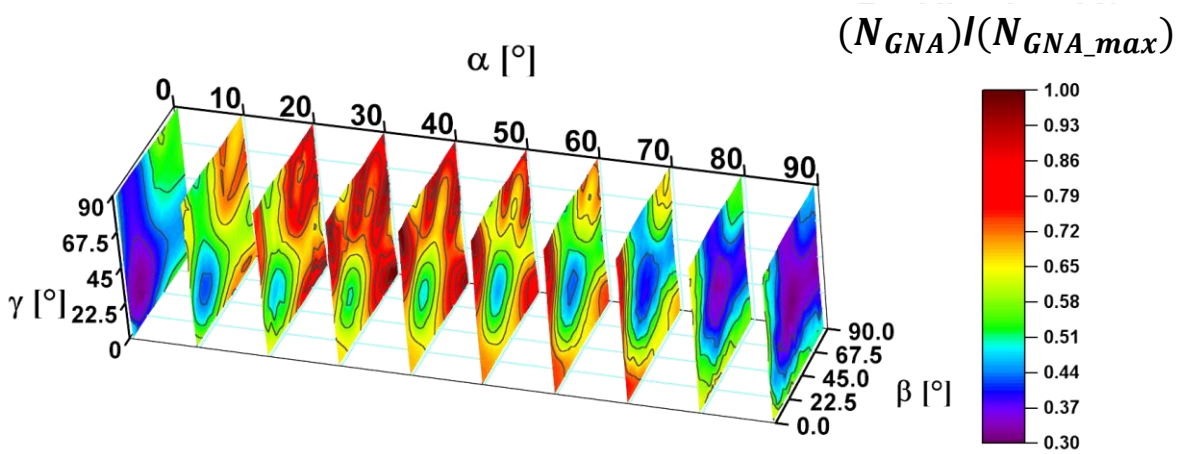

Fig. 19: Buckling load N_{GNA} of the perfect shell structure for different laminate stacking sequences normalized to the maximum perfect buckling load

In Fig. 19 the normalized buckling load N_{GNA} is shown for composite cylindrical shells with different laminate stacking sequences. All buckling loads were normalized to the maximum perfect buckling load and a color close to dark red indicates the laminate stacking sequences with the highest buckling load of the perfect shell. The results show that there are several regions with high buckling loads. Especially, in a range of α = 20-40, β and γ = 0 & 90 which corresponds to quasi-isotropic behavior for example [45,-45, 0, 90]s.

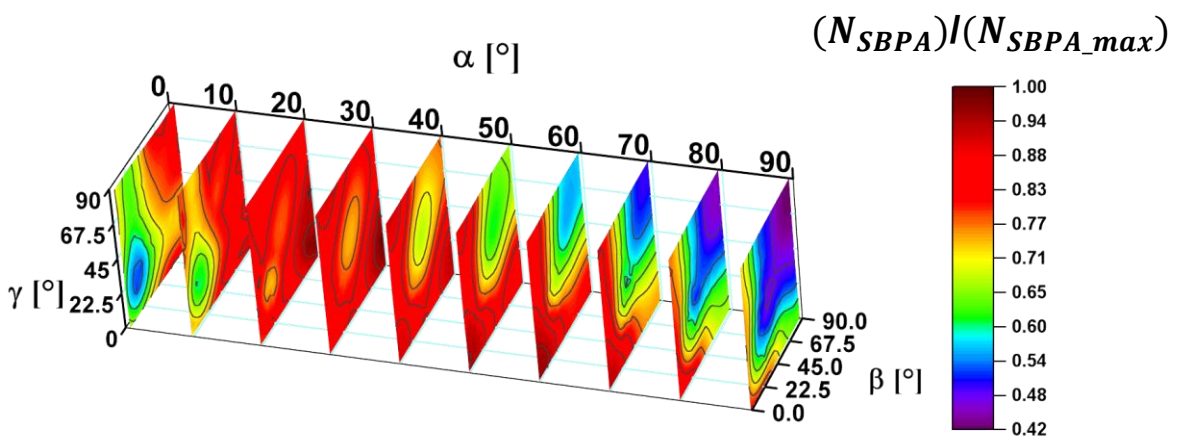

Fig. 20: Buckling load N_{SBPA} for different laminate stacking sequences normalized to the maximum lower-bound buckling load

The results of the SBPA iteration are shown in Fig. 20 and the maximum imperfect buckling loads also correspond to quasi-isotropic behavior or slightly more axially-stiff shells like [±60,0,0]s. The highest imperfect buckling load can be identified at $[\pm 25, 90, 15]_s$ and the highest perfect buckling load can be identified at [±40, 5, 85]s. Other stacking sequences which may result in a high performance cylinder are summarized in Table 5.

Table 5: Laminate stacking sequence for high performance cylinders

ply-layup	N_{GNA} [kN]	N_{SBPA} [kN]	A_{11}/A_{22}	$\underline{A}_{66}$	D_{11}/D_{22}	$\underline{D}_{66}$
$[\pm 25,90,15]s$	114.80	92.59	1.81	0.08	3.07	0.18
$[\pm 30,90,0]s$	161.91	87.79	1.68	0.08	2.34	0.26
$[\pm 40,5,85]s$	173.14	83.91	1.21	0.12	1.93	0.44
$[\pm 45,90,0]s$	143.55	83.12	1	0.12	0.78	0.44
$[\pm 45,0,90]s$	159.65	85.31	1	0.12	1.28	0.44
$[\pm 60,0,0]s$	121.03	87.97	1.68	0.08	0.46	0.25

4.2 Application of machine learning

4.2.1 Decision tree-based machine learning

Within this article the scikit-learn decision tree classifier [77], [78] was used and in the following a brief description for this approach is given. For a more detailed overview regarding machine learning the book by Witten [79] is recommended.
A decision tree is based on the hierarchical tree-like partition of the input data (in this case the stiffness ratios and the buckling loads). The purpose of this method is to create a model which predicts the values of target variables based on several input features. The decision tree is defined as a regression tree if the target variable is continuous and as a classification tree if the target variable is discrete. In this case, the target variable (buckling load) is discrete and two classes were defined for the classification tree. The class 1 corresponds to a high buckling load (in this example, class 1 $\geq$ 32 kN) and the class 0 corresponds to the remaining buckling loads (class 0 $<$ 32 kN), see Fig. 21.

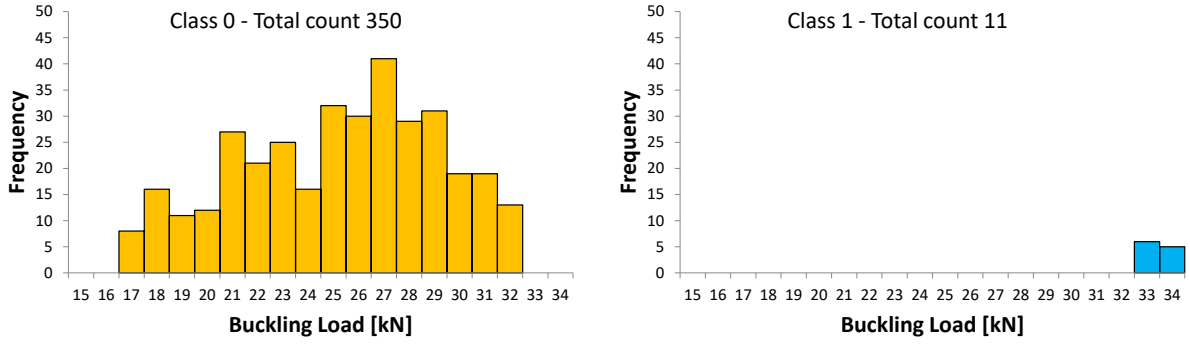

Fig. 21: Histogram for the composite cylinders from section 3: class 0 buckling loads (left) class 1 buckling loads (right)

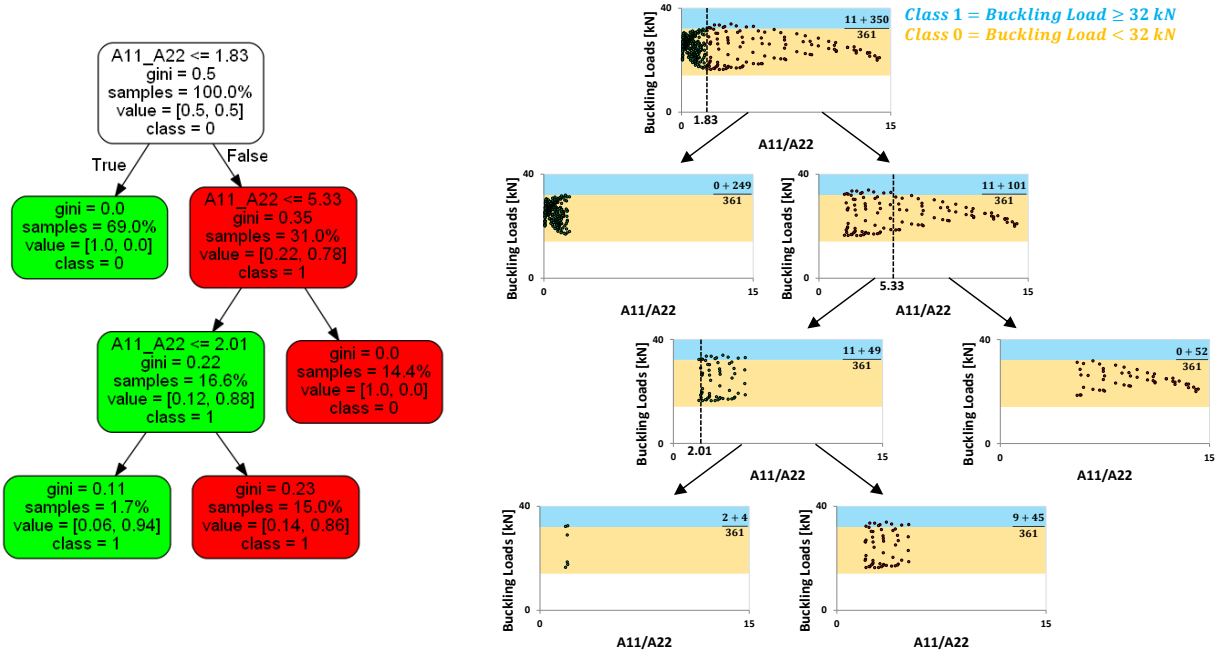

Fig. 22: Example of a classification tree for the buckling load of composite cylinders under axial compression

An example for a corresponding classification tree is shown in Fig. 22. The classification tree consists of internal nodes and leaf nodes. Each internal node (or decision node) has two or more branches and represents a test on a feature (true or false – corresponding to green or red in Fig. 22 - left). The topmost decision node in a tree corresponds to the best predictor and is called root node. The leaf nodes represent a classification or decision.
The decisions of the classification tree are based on the gini impurity criterion [79] which measures how often a randomly chosen element from the set would be incorrectly labeled if it was randomly labeled according to the distribution of labels in the subset. As the gini impurity is a probability its values is between 0 and 1. The decision tree algorithm will construct the tree such that the gini impurity is most minimized. An illustrative example for a decision tree is given in Fig. 22 (right). This specific example shows that the A_{11}/A_{22} ratio should be between 1.83 and 2.01 in order to have a high probability of having a class 1 buckling load.

4.2.2 Results for maximum buckling load cylinders

This section summarizes the results of the decision tree algorithm for the design of composite cylinder with a high buckling load. The stiffness ratios (membrane, bending, in-plane shear and twisting stiffnesses) for a composite shell without imperfection (perfect shell) and the corresponding design limits are shown in Fig. 23 - Fig. 24 and given by equation (6).

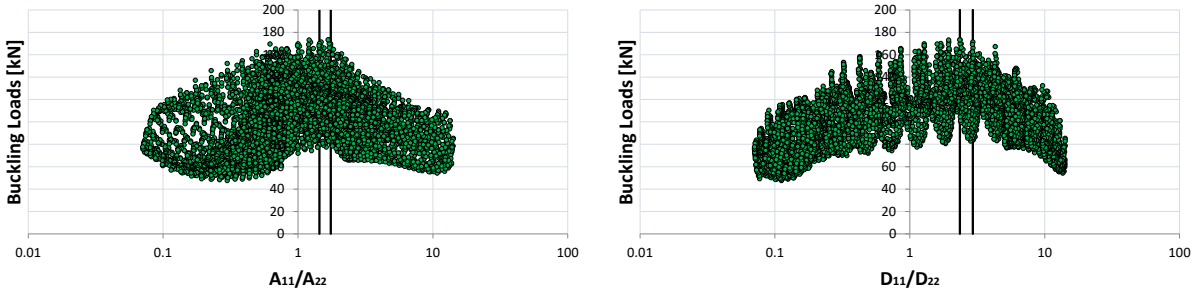

Fig. 23: Buckling load (perfect) vs. axial-to-circumferential membrane stiffness ratio (A_{11}/A_{22}) – left – and bending stiffness ratio (D_{11}/D_{22}) – right – for the $[\pm\alpha,\beta,\gamma,\gamma,\beta,\mp\alpha]$ shells

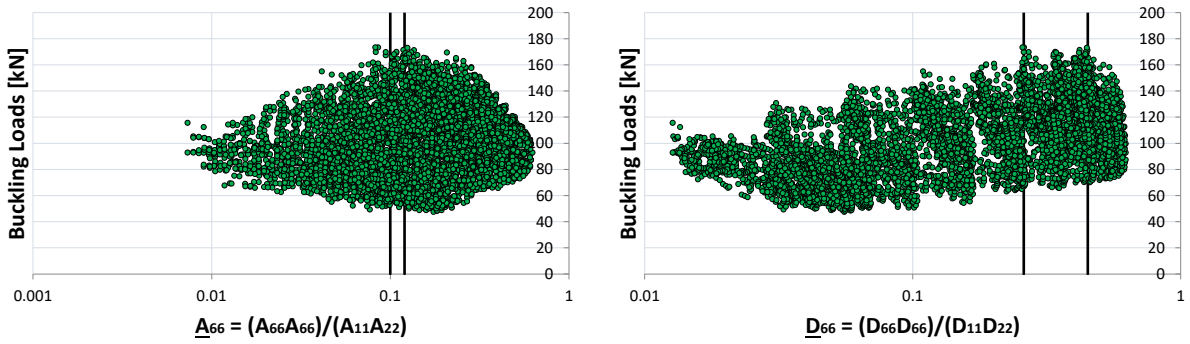

Fig. 24: Buckling load (perfect) vs. in-plane shear stiffness to axial and circumferential membrane stiffness – left – and in-plane twisting stiffness to axial and circumferential bending stiffness – right – for the [±α,β,γ,γ,β,∓α] shells

$$
\begin{aligned}
1.44 \leq \frac{A_{11}}{A_{22}} \leq 1.75 \\
2.35 \leq \frac{D_{11}}{D_{22}} \leq 2.93 \\
0.10 \leq \underline{A}_{66} \leq 0.12 \\
0.26 \leq \underline{D}_{66} \leq 0.45
\end{aligned}
\tag{6}
$$

4.2.3 Results for maximum buckling load and minimum imperfection sensitivity cylinders

This section summarizes the results of the decision tree algorithm for the design of composite cylinder with a high buckling load and a low imperfection sensitivity. The stiffness ratios (membrane, bending, in-plane shear and twisting stiffnesses) for a composite shell with imperfection (lower-bound) and the corresponding design limits are shown in Fig. 25 - Fig. 26 and given by equation (7).

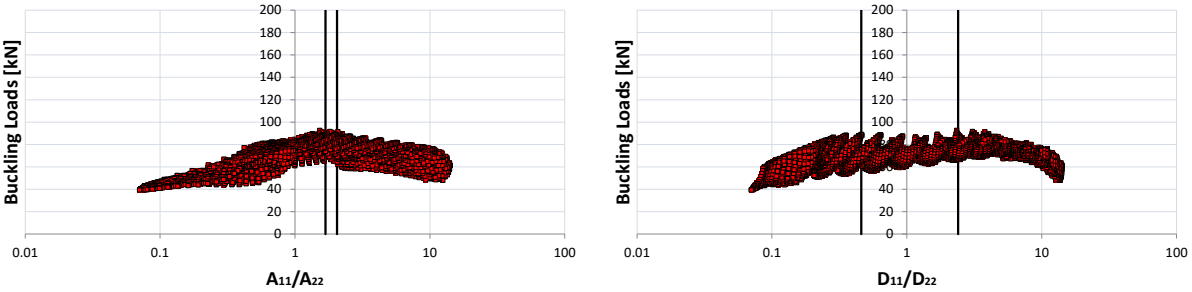

Fig. 25: Buckling load (imperfect - SBPA) vs. axial-to-circumferential membrane stiffness ratio (A_{11}/A_{22}) – left – and bending stiffness ratio (D_{11}/D_{22}) – right – for the [±α,β,γ,γ,β,∓α] shells

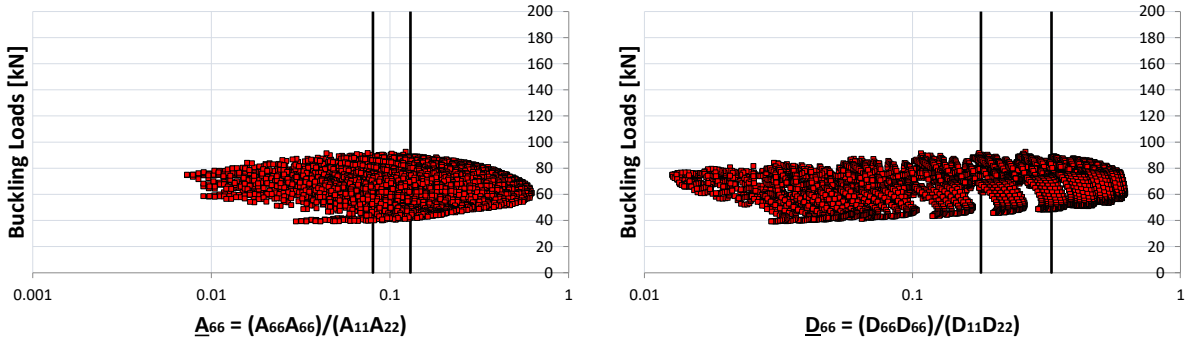

Fig. 26: Buckling load (imperfect - SBPA) vs. in-plane shear stiffness to axial and circumferential membrane stiffness – left – and in-plane twisting stiffness to axial and circumferential bending stiffness – right – for the [±α,β,γ,γ,β,∓α] shells

$$
\begin{aligned}
1.68 \leq \frac{A_{11}}{A_{22}} \leq 2.05 \\
0.46 \leq \frac{D_{11}}{D_{22}} \leq 2.40 \\
0.08 \leq \underline{A}_{66} \leq 0.13 \\
0.18 \leq \underline{D}_{66} \leq 0.33
\end{aligned}
\tag{7}
$$

5 Practical application

In this section, the design recommendations from section 4.2 are used to generate composite cylinders with:

1. Maximum buckling load
2. Maximum buckling load and a minimum imperfection sensitivity

The laminate stacking sequences which will be analyzed are based on studies by Zimmerman [52] and have a [α,–α,β,–β,γ,–γ,δ,–δ,ε,–ε] sequence. The investigated shells have a radius R = 250 mm, a free length L = 500 mm, a wall thickness t = 1.25 mm and a ply thickness of t_{ply} = 0.125 mm. The material parameters are given in Table 6.

Table 6: Material properties of the investigated cylindrical shells after [52]

Material parameter	**Dimension**
elasticity modulus E_{11} - [MPa]	123551
elasticity modulus E_{22} - [MPa]	8708
Poisson's ratio ν_{12} - [-]	0.32
shear modulus G_{12} - [MPa]	5695

Zimmerman generated laminate stacking sequences which led to composite cylinders with a buckling load between approximately 98 kN and 260 kN. The corresponding laminate stacking sequence for the maximum buckling load composite cylinder is given in Table 7.

Table 7: Material properties of the investigated cylindrical shells after [52]

Laminate Stacking	**Reference**	**Buckling Load [kN]**
		Perfect shell (GNA)
[30,-30,90,-90,22,-22,38,-38,53,-53]	Zimmerman [52]	260.60
[38,-38,68,-68,90,90,90,90,38,-38]	Friedrich [68]	252.93
[25,-25,25,-25,85,-85,0,0,50,-50]	Opti.-perfect	264.01
[60,-60,0,0,0,0,30,-30,60,-60]	Opti.-imperfect	217.76

The design limits from section 4.2.2 and 4.2.3 were used to generate ply layups for the [α,–α,β,–β,γ,–γ,δ,–δ,ε,–ε] laminate. The ply angles are varied in 5°-steps from 0°-90° which may result in about 2.5 million different ply layups. The requirements for a maximum buckling load according to equation 6 are fulfilled by 118 configurations as shown in Fig. 27. A histogram for the corresponding calculated buckling loads is given in and the laminate stacking for the maximum buckling load is given in Table 7.

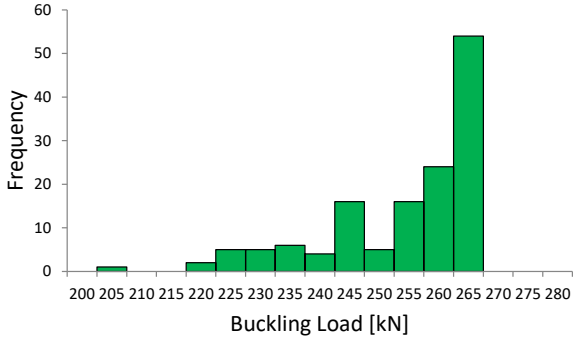

Fig. 27: Histogram for the maximum buckling load cylinders which fulfil the requirements of equation (6)

The average buckling load of all 118 configurations is 251 kN which is very close to the maximum buckling load for this type of laminate configuration (264 kN). This result indicates that the design limits from section 4.2 are suitable for general design recommendations.
Next, the laminate configurations with a maximum buckling load and a minimum imperfection sensitivity are generated. In this case, the requirements for a maximum buckling load and a minimum imperfection sensitivity according to equation 7 are fulfilled by 5922 configurations. Due to the large number of configurations, the laminate stacking with the maximum perfect buckling load from a sample of about 118 shells was chosen. The corresponding configuration has a [60,-60, 0, 0, 0, 0, 30,-30, 60,-60] stacking sequence and is compared with a laminate by Friedrich et al. [80] which was also designed for maximum buckling load and minimum imperfection sensitivity.
The load-displacement curves for the composite cylinders with the laminate stacking from Table 7 by Zimmerman, Friedrich and this study are shown in Fig. 28.

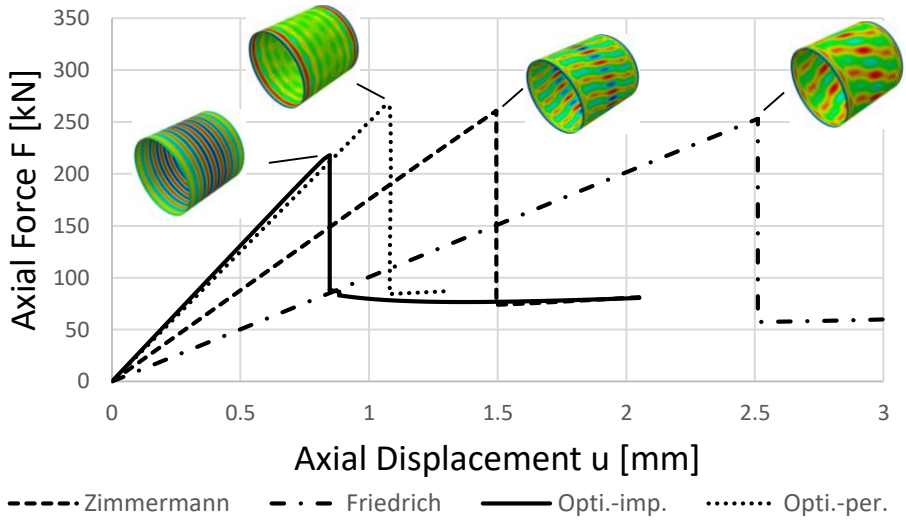

Fig. 28: Load-displacement curve of different composite shells with 5 different plies angles

The shells by Zimmerman and Friedrich have a significantly less axial stiffness compared to the shells from this article. As in the previous section 3, different imperfections were applied to determine imperfect buckling loads for these shells and the corresponding results are shown in Fig. 29 and given in Table 8.

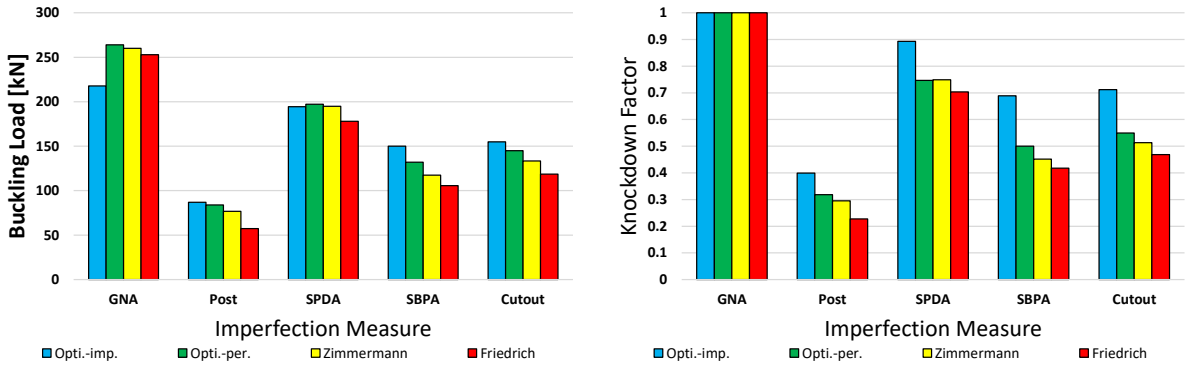

Fig. 29: Comparison of the buckling load and KDF for composite cylinders (with 5 different ply angles) under axial compression with optimized stacking sequences from literature

The results show that the shells which were designed according to the stiffness ratio limits from section 4.2 outperform the composite cylinders by Zimmerman and Friedrich in every case. The

shell Opti.-imp. has always the lowest imperfection sensitivity (highest KDF) and also the highest imperfect buckling loads (except for the SPDA). The shell design by Friedrich has the worst overall performance.

Table 8: Comparison of optimized stacking sequences (with 5 different ply angles) burdened by different imperfections with corresponding buckling loads in [kN]

Shell	Opti.-per.	Opti.-imp.	Zimmerman [52]	Friedrich [68]
Perfect shell (GNA)	**264.01**	217.76	260.60	252.93
Postbuckling	84.04	**87.23**	76.71	57.43
SPDA	**197.20**	194.50	194.90	178.00
SBPA	132.57	**150.03**	117.40	105.84
Cutout	145.13	**155.32**	132.31	118.51
Best	2 times	3 times	0 times	0 times

6 Conclusion and Outlook

The purpose of this article is to derive general design recommendations for the laminate stacking sequence of high-performance (high buckling load and low imperfection sensitivity) composite cylinder under axial compression.
In the first step, the numerical model and state-of-the-art imperfection modeling techniques were presented and described in detail. The influence of different imperfection types on an academic laminate stacking sequences with 2 different ply angles was investigated. Based on the results of section 3, it was decided to use the perfect buckling load and the imperfect buckling load according to the SBPA as basis for an optimization using brute force.
A multi-objective optimization for maximum buckling load and minimum imperfection sensitivity of composite cylinder under axial compression with 3 different ply angles is performed. The results of this optimization are used as input data for a machine learning algorithm in order to derive general design recommendations which are based on the relative membrane, bending, in-plane shear and twisting stiffnesses. Subsequently, several optimal laminate stacking sequences are generated and compared with similar laminate configurations from literature. The results show that the design recommendations of this article lead to high-performance cylinders which outperform comparable composite shells considerably. The results of this article may be the basis for future lightweight design of sandwich and monolithic composite cylinders of modern launch-vehicle primary structures.

Acknowledgement:

The work presented was reviewed by Dr. Marc Robert Schultz from the NASA Langley Research Center. His helpful comments and corrections are gratefully acknowledged.

Appendix A

In this section the decision tree for the perfect shell analysis (Fig. 30) and the imperfect shell analysis (Fig. 31) from section 4.2 are given.

Fig. 30: Decision Tree for the perfect shell

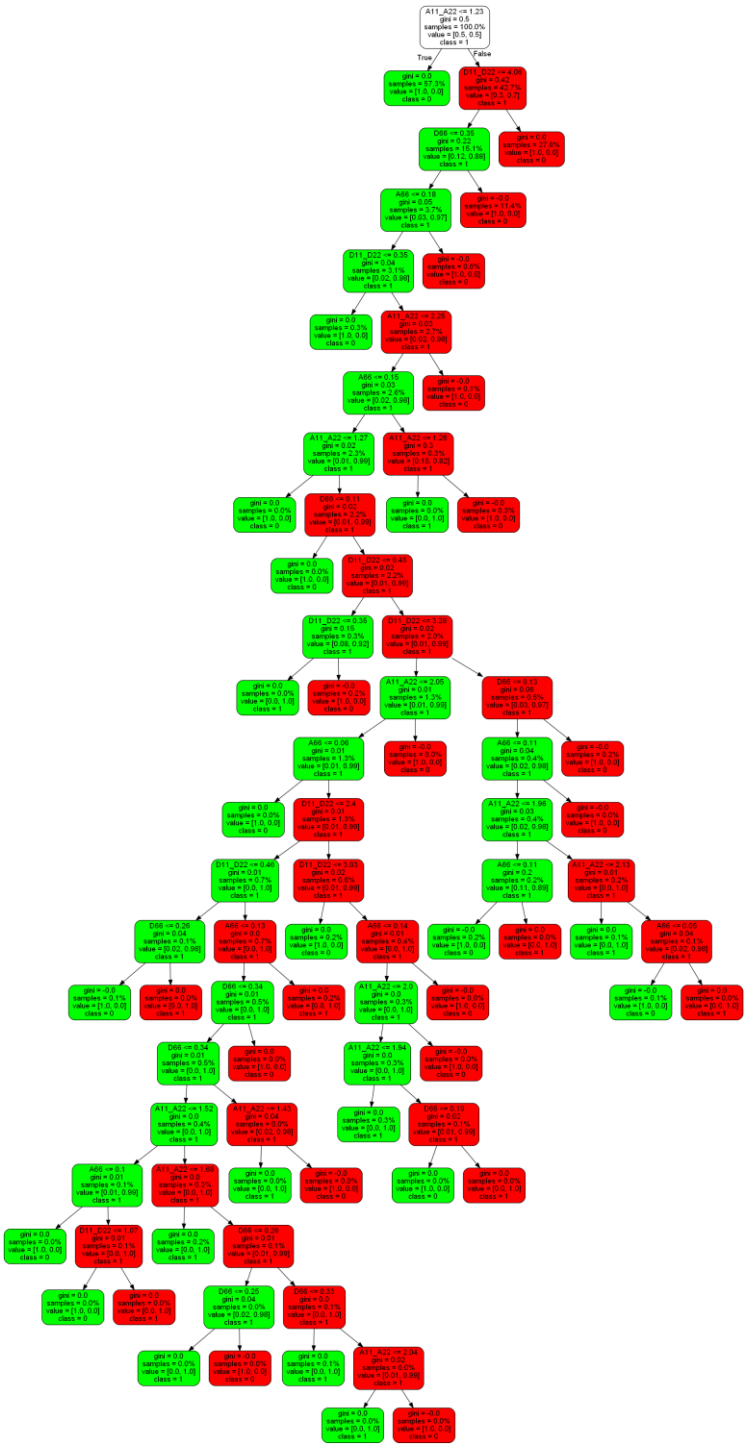

Fig. 31: Decision Tree for the imperfect shell

7 References

[1] M. H. Hilburger and J. H. J. and Starnes, "High-fidelity Analysis of Compression-loaded Composite Shells," *Proceedings of the 42st AIAA/ASME/ASCE/AHS/ASC Structures, Structural Dynamics, and Materials Conference,* pp. AIAA Paper No. 2001-1394, 2001.

[2] H. Abramovich, Stability and Vibrations of Thin Walled Composite Structures, Elsevier Science & Technology ; Woodhead Publishing, 2017.

[3] M. Schultz and M. Nemeth, "Buckling Imperfection Sensitivity of Axially compressed orthotropic cylinders".*51st AIAA/ASME/ASCE/AHS/ASC Structures, Structural Dynamics, and Materials Conference
18th 12 - 15 April 2010, Orlando, Florida.*

[4] M. R. Schultz, D. W. Sleight, D. E. Myers, W. A. J. Waters, P. B. Chunchu, A. W. Lovejoy and M. W. Hilburger, "Buckling Design and Imperfection Sensitivity of Sandwich Composite Launch-Vehicle Shell Structures," *Conference: Proceedings of the American Society for Composites: Thirty-First Technical Conference, At Williamsburg, VA,* 2016.

[5] W. T. Koiter, *The Stability of Elastic Equilibrium [PhD thesis] - 1945 [in Dutch],* TH Delft, Ed., Englisch Translation NASA TTF-10; 1967, p. 1–833.

[6] H. Wagner, E. Sosa, C. Hühne, T. Ludwig, J. Croll and R. Khakimova, "ROBUST DESIGN OF IMPERFECTION SENSITIVE THIN-WALLED SHELLS UNDER AXIAL COMPRESSION, BENDING OR EXTERNAL PRESSURE – APPLICATION AND VALIDATION," *International Journal of mechanical sciences, 2019, accepted manuscript.*

[7] H. Wagner, E. Petersen and C. Hühne, "BUCKLING ANALYSIS OF AN AXIALLY LOADED HIGH PERFORMANCE HYBRID COMPOSITE CYLINDER – EXPERIMENTAL TESTING AND SIMULATION," *Composite Structures, 2019, accepted manuscript.*

[8] H. Wagner and C. R. K. Hühne, "Towards robust knockdown factors for the design of conical shells under axial compression".*International Journal of Mechanical Sciences, 2018, Vol. 146-147, pp. 60-80.*

[9] H. Wagner, C. Hühne and S. Niemann, "Robust knockdown factors for the design of spherical shells under external pressure: Development and validation," *International Journal of Mechanical Sciences, Volume 141, 2018, Pages 58-77.*

[10] H. Wagner, C. Hühne, J. Zhang and W. Tang, "GEOMETRIC IMPERFECTION AND LOWER-BOUND ANALYSIS OF SPHERICAL SHELLS UNDER EXTERNAL PRESSURE," *Thin-walled Structures, 2019, accepted manuscript.*

[11] M. Hilburger, M. Nemeth and J. J. Starnes, "Shell Buckling Design Criteria Based on Manufacturing Imperfection Signatures," *NASA/TM-2004-212659,* 2004.

[12] D. B. Muggeridge and R. C. Tennyson, "Buckling of axisymmetric imperfect circular cylindrical shells underaxial compression," *AIAA Journal,* vol. 7, p. 2127–2131, 1969.

[13] J. Arbocz, "The imperfections data bank, a means to obtain realistic buckling loads," *In Ramm E. Buckling of shells,* 1982.

[14] C. Hühne, R. Rolfes and J. Teßmer, "A new approach for robust design of composite cylindrical shells under axial compression," in *Proceedings of the European Conference on Spacecraft Structures*, 2005.

[15] C. Hühne, R. Rolfes, E. Breitbach and J. Teßmer, "Robust design of composite cylindrical shells under axial compression — Simulation and validation," *Thin-Walled Structures,* vol. 46, p. 947–962, 2008.

[16] B. Wang, X. Ma, H. Pang, Y. Sun, K. Tian, G. Li, K. Zhang, L. Jiang and J. Guo, "Improved knockdown factors for composite cylindrical shells with delamination and geometric imperfections," *Composites Part B: Engineering, Vol. 163, 2019, pp. 314-323.*

[17] C. Hühne, R. Zimmermann, R. Rolfes and B. Gier, Loading imperfections – Experiments and computations, Euromech colloquium 424, 2001.

[18] C. Hühne, R. Zimmermann, R. Rolfes and B. Geier, "SENSITIVITIES TO GEOMETRICAL AND LOADING IMPERFECTIONS ON BUCKLING OF COMPOSITE CYLINDRICAL SHELLS," *In Proceedings of European Conference on Spacecraft,* 2002.

[19] R. Wagner and C. Hühne, "A NEW DESIGN CONCEPT FOR CYLINDRICAL COMPOSITE SHELLS UNDER AXIAL COMPRESSION," in *Proceedings of the European Conference on Composite Materials - ECCM16*, Sevillia, Spain, 2014.

[20] H. Wagner, C. Hühne and S. Niemann, "Constant Single-Buckle Imperfection Principle to determine a lower bound for the buckling load of unstiffened composite cylinders under axial compression," *Composite Structures,* vol. 139, pp. 120-129, 2016.

[21] M. W. Hilburger, A. E. Lovejoy, R. P. Thornburgh and C. Rankin, "Design and Analysis of Subscale and Full-Scale Buckling-Critical Cylinders for Launch Vehicle Technology Development," *AIAA Paper 2012-1865, NF1676L-13285,* 2012.

[22] M. W. Hilburger, W. T. Haynie, A. E. Lovejoy, M. G. Roberts, J. P. Norris, W. A. Waters and H. M. Herring, "Subscale and Full-Scale Testing of Buckling-Critical Launch Vehicle Shell Structures," *AIAA Paper 2012-1688, NF1676L-13284.*

[23] M. W. Hilburger, W. A. J. Waters and W. T. Haynie, "Buckling Test Results from the 8-Foot-Diameter Orthogrid-Stiffened Cylinder Test Article TA01. [Test Dates: 19-21 November 2008]," *NASA/TP-2015-218785, L-20490, NF1676L-20067,* 2015.

[24] M. W. Hilburger, W. A. J. Waters, W. T. Haynie and R. P. Thornburgh, "Buckling Test Results and Preliminary Test and Analysis Correlation from the 8-Foot-Diameter Orthogrid-Stiffened Cylinder Test Article TA02," *NASA/TP-2017-219587, L-20801, NF1676L-26704,* 2017.

[25] M. Schultz, D. Sleight, N. Gardner, M. Rudd, M. Hilburger, T. Palm and N. Oldfield, "Test and Analysis of a Buckling-Critical Large-Scale Sandwich Composite Cylinder," *2018 AIAA/ASCE/AHS/ASC Structures, Structural Dynamics, and Materials Conference, AIAA SciTech Forum, (AIAA 2018-1693).*

[26] M. R. Schultz, D. W. Sleight, D. E. Myers, W. A. Waters, P. B. Chunchu, A. W. Lovejoy and M. W. Hilburger, "Buckling Design and Imperfection Sensitivity of Sandwich Composite Launch-Vehicle Shell Structures," *Conference: Proceedings of the American Society for Composites: Thirty-First Technical Conference, At Williamsburg, VA,* 2016.

[27] "SBKF. NASA shell buckling knockdown factor project; 2017. Available from:<https://www.nasa.gov/offices/nesc/home/Feature_ShellBuckling_Test.html> [cited 2017 11-05-2017]".

[28] M. Hilburger, "Developing the next generation shell buckling design factors and technologies," *53rd AIAA/ASME/ASCE/AHS/ASC structures, structural dynamics and materials conference, Honolulu; 2012.*

[29] M. W. Hilburger, "On the Development of Shell Buckling Knockdown Factors for Stiffened Metallic Launch Vehicle Cylinders," *2018 AIAA/ASCE/AHS/ASC Structures, Structural Dynamics, and Materials Conference.*

[30] M. Hilburger, M. C. Lindell, W. A. Waters and N. W. Gardner, "Test and Analysis of Buckling-Critical Stiffened Metallic Launch Vehicle Cylinders," *2018 AIAA/ASCE/AHS/ASC Structures, Structural Dynamics, and Materials Conference.*

[31] R. Degenhardt, R. Zimmermann, A. Kling and D. Wilckens, "New Robust Design Guideline for imperfection sensitive composite launcher structures," in *3rd CEAS Congress*, Venice, Italy, 2011.

[32] R. Khakimova, C. Warren, R. Zimmerman, S. Castro and R. Degenhardt, "The single perturbation load approach applied to imperfection sensitive conical composite structures," *Thin-Walled Structures,* vol. 84, pp. 369-377, 2014.

[33] R. Degenhardt, A. Bethge, A. Kling, R. Zimmermann and K. Rohwer, "Probabilistic approach for improved buckling knock-down factors of CFRP cylindrical shells," in *Proceeding of 18th Engineering Mechanics Division Conference*, 2007.

[34] E. Skukis, O. Ozolins, K. Kalnins and M. Arbelo, "Experimental Test for Estimation of Buckling Load on Unstiffened Cylindrical shells by Vibration Correlation Technique," *Procedia Engineering,* vol. 172, pp. 1023-1030, 2017.

[35] E. Skukis, K. Kalnins and O. Ozolins, "Application of Vibration Correlation Technique for Open Hole Cylinders," *Nonlinear Dynamics–2016 (ND-KhPI2016) : proceedings of 5th International Conference, dedicated to the 90th anniversary of Academician V. L. Rvachev,* pp. 377-383, 2016.

[36] R. Degenhardt, A. Kling, R. Zimmermann and F. Oderman, Dealing with imperfection sensitivity of composite structures prone to buckling, in "Advances in Computational Stability Analysis" ; book edited by Safa Bozkurt Coskun, ISBN 978-953-51-0673-9, 2012.

[37] R. Khakimova, S. Castro, D. R. K. Wilckens and R. Degenhardt, "Buckling of axially compressed CFRP cylinders with and without additional lateral load: Experimental and numerical investigation," *Thin-Walled Structures,* vol. 119, pp. 178-189, 2017.

[38] R. Khakimova, R. Zimmermann, D. Wilckens, K. Rohwer and R. Degenhardt, "Buckling of axially compressed CFRP truncated cones with additional lateral load: Experimental and numerical investigation," *Composite Structures,* vol. 157, pp. 436-447, 2016.

[39] R. Khakimova, D. Wilckens, J. Reichardt and R. Degenhardt, "Buckling of axially compressed CFRP truncated cones: Experimental and numerical investigation," *Composite Structures,* vol. 146, pp. 232-247, 2016.

[40] D. Sleight, A. Satyanarayana and M. R. Schultz, "Buckling Imperfection Sensitivity of Conical Sandwich Composite Structures for Launch-Vehicles," *2018 AIAA/ASCE/AHS/ASC Structures, Structural Dynamics, and Materials Conference.*

[41] R. Khakimova, "Ply topology based design concept for composite truncated cones manufactured by tape laying".*DIssertation, TU-Braunschweig, 2017.*

[42] I. Balbin, C. Bisagni, M. Schultz and M. Hilburger, "Scaling Methodolgy for buckling of sandwich composite cylindrical structures," *2018 AIAA/ASCE/AHS/ASC Structures, Structural Dynamics, and Materials Conference, AIAA SciTech Forum, (AIAA 2018-1693).*

[43] H. Wagner and C. Hühne, "Robust knockdown factors for the design of cylindrical shells under axial compression: potentials, practical application and reliability analysis," *International Journal of Mechanical Sciences 135,* pp. 410-430, 2018.

[44] P. Hao, B. Wang, G. Li, Z. Meng, K. Z. Tian and X. Tang, "Worst Multiple Perturbation Load Approach of stiffened shells with and without cutouts for improved knockdown factors," *Thin-Walled Structures,* vol. 82, pp. 321-330, 2014.

[45] K. Tian, B. Wang, P. Hao and A. Waas, "A high-fidelity approximate model for determining lower-bound buckling loads for stiffened shells".*In International Journal of Solids and Structures, 2017, ISSN 0020-7683, https://doi.org/10.1016/j.ijsolstr.2017.10.034.*

[46] H. Wagner, Hühne, S. Niemann and R. Khakimova, "Robust design criterion for axially loaded cylindrical shells - Simulation and Validation," *Thin-Walled Structures; Vol. 115, pp. 154-162, http://dx.doi.org/10.1016/j.tws.2016.12.017,* 2017.

[47] H. Wagner, C. Hühne, S. Niemann and L. Weiß, "High-fidelity design methods to determine knockdown factors for the buckling load of axially loaded composite cylindrical shells".*Proceedings of the 11th International Conference Shell Structures - Theory and Applications, (Ssta 2017), October 11-13, 2017, Gdansk, Poland.*

[48] H. Wagner, C. Hühne, S. Niemann, K. Tian, B. Wang and P. Hao, "Robust knockdown factors for the design of cylindrical shells under axial compression: Analysis and modeling of stiffened and unstiffened cylinders," *Thin-walled structures 127, 629-645, 2018.*

[49] H. Wagner, C. Hühne, K. Rohwer, S. Niemann and M. Wiedemann, "Stimulating the realistic worst case buckling scenario of axially compressed cylindrical composite shells," *Composite Structures,* vol. 160, pp. 1095-1104, 2017.

[50] H. Wagner, C. Hühne and S. Niemann, "Robust knockdown factors for the design of axially loaded cylindrical and conical composite shells - Development and Validation," *Composite Structures,* vol. 173, no. 10.1016/j.compstruct.2017.02.031, pp. 281-303, 2017.

[51] A. Evkin, "Local buckling of cylindrical shells - Pogorevlov's geometrical method," *Special Issue: Problems of Nonlinear Mechanics and Physics of Materials , April 2018, Springer-Verlag.*

[52] R. Zimmerman, "Buckling Resaerch for imperection Tolerant Fiber Composite Structures," *In: Spacecraft Structures, Materials and Mechanical Engineering, Proceedings of the Conference held by ESA, CNES and ARA in Norrdwijk, 27-29 March 1996.*

[53] R. Tennyson and J. Hansen, "Optimum design for buckling of laminated cylinders," *In: Collapse: The buckling of structures in theory and practice; Symposium, University College, London, 13 Aug. to 3. Sept., 1982, pp. 409-427.*

[54] D. Bushnell, "Computerized Buckling Analysis of Shells," *Final Report AFWAL TR 81-3049, Flight Lockheed Palo Alto Research Laboratory, 1981.*

[55] H.-R. Meyer-Piening, M. Farshad, B. Geier and R. Zimmermann, "Buckling Loads of CFRP composite cylinders under combined axial and torsion loading - experiments and computations," *Composite Structures,* vol. 53(4), pp. 427-435, 2001.

[56] B. Geier, H.-R. Meyer-Piening and R. Zimmermann, "On the influence of laminate stacking on buckling of composite cylindrical shells subjected to axial compression," *Composite Structures,* vol. 55, p. 467–474, 2002.

[57] N. Khot and V. Venkayya, "Effect of fiber orientation on initial postbuckling behavior and imperefction sensitivity of composite cylindrical shells," *Technical Report AFFDL-TR-70-125, Air Force Flight Dynamics Laboratory,* 1970.

[58] R. C. Tennyson and J. S. Hansen, "Optimum Design for Buckling of Laminated Cylinders," *Collapse: The Buckling of Structures in Theory and Practice, Cambridge University Press, Cambridge,* 1983.

[59] Y. Hirano, "Optimization of Laminated Composite Cylindrical Shells for Axial Buckling," *J. Jpn. Soc. Aeronaut. Space Sci.,* vol. 32(360), p. 46–51, 1984.

[60] J. Onoda, "Optimal Laminate Configurations of Cylindrical Shells for Axial Buckling," *AIAA Journal, 1985, Vol. 23, No. 7.*

[61] Y. Nshanian and M. Pappas, "Optimal Laminated Composite Shells for Buckling and Vibration," *AIAA Journal, 1983, Vol. 21, No. 3.*

[62] A. Todoroki and T. Ishikawa, "Design of experiments for stacking sequence optimizations with genetic algorithm using response surface approximation," *Composite Structures 64, (2004), 349–357.*

[63] C. Hühne, "Robuster Entwurf beulgefährdeter, unversteifter Kreiszylinderschalen aus Faserverbund," *PhD Thesis at Technische Universität Carolo-Wilhelmina zu Braunschweig,* 2006.

[64] I. Elishakoff, B. Kriegesmann, R. Rolfes, C. Hühne and A. Kling, "Optimization and antioptimization of buckling load for composite cylindrical shells under uncertainties," *AIAA Journal,* vol. 50(7), pp. 1513-1524, 2012.

[65] *Dassault Systems, ABAQUS 6.13—Software Package, 2013.*

[66] L. Wullschleger and H. R. Meyer-Piening, "Buckling of geometrically imperfect cylindrical shells - definition of a buckling load," *International Journal of Non-Linear Mechanics,* vol. 37, pp. 645-657, 2002.

[67] B. Kriegesmann, R. Rolfes, E. Jansen, I. Elishakoff, C. Hühne and A. Kling, "Design optimization of composite cylindrical shells under uncertainty," *CMC, Vol. 32, no 3, pp 177-200, 200.*

[68] L. Friedrich, S. Loosen, K. Liang, M. Ruess, C. Bisagni and K. Schröder, "Stacking sequence influence on imperfection sensitivity of cylindrical composite shells under axial compression," *Composite Structures 134, pp 750-761, 2015.*

[69] B. Wang, S. Zhu, P. Hao, X. Bi, K. Du, B. Chen, X. Ma and Y. Chao, "Buckling of Quasi-Perfect Cylindrical Shell under Axial Compression: A Combined Experimental and Numerical Investigation," *International Journal of Solids and Structures; In Press, Accepted Manuscript; https://doi.org/10.1016/j.ijsolstr.2017.09.029.*

[70] B. Wang, K. Du, H. Peng, K. Tian, Y. Chai, L. Jiang, S. Xu and X. Zhang, "Experimental validation of cylindrical shells under axial compression for improved knockdown factors," *International Journal of Solids and Structures, 2019, accepted manuscript.*

[71] T. Ludwig, C. Hühne and L. De Lorenzis, "Rotation-free Bernstein-Bézier elements for thin plates and shells – development and validation," *Computer Methods in Applied Mechanics and Engineering, 2019, accepted manuscript.*

[72] J. J. Starnes, "The effect of cutouts on the buckling of thin shells," *Thin shell structures, Theory, experiment and design, Y.C. Fung and E.E. Sechler, eds., Prentice-Hall, Englewood Cliffs, N.J., 1974, 289-304.*

[73] H. Wagner, Robust Design of Buckling Critical Thin-Walled Shell Structures, PhD Thesis, Technical University Carolo-Wilhelmina, Braunschweig, 2018.

[74] I. Elishakoff, "Probabilistic resolution of the twentieth century conundrum in elastic stability," *Thin-Walled Structures,* vol. 59, pp. 35-57, 2012.

[75] I. Elishakoff, "Resolution of the Twentieth Century Conundrum in Elastic Stability," *Singapore: World Scientific, 2014.*

[76] M. Eßlinger, "Hochgeschwindigkeitsaufnahmen vom Beulvorgang dünnwandiger, axialbelasteter Zylinder," *Der Stahlbau,* vol. 39, p. 73–76, 1970.

[77] "https://scikit-learn.org/stable/index.html," [Online].

[78] "https://hackernoon.com/a-brief-look-at-sklearn-tree-decisiontreeclassifier-c2ee262eab9a," [Online].

[79] I. Witten, E. Frank, M. Hall and C. Pal, Data Mining, Practical Machine Learning Tools and Techniques, Morgan Kaufmann, 2016.

[80] L. Friedrich, P. Lyssakow, G. Pearce, M. Ruess, C. Bisagni and K. Schroeder, "ON THE STRUCTURAL DESIGN OF IMPERFECTION SENSITIVE LAMINATED COMPOSITE SHELL STRUCTURES SUBJECTED TO AXIAL COMPRESSION," *ECCOMAS Congress 2016, VII European Congress on Computational Methods in Applied Sciences and Engineering, M. Papadrakakis, V. Papadopoulos, G. Stefanou, V. Plevris (eds.).*